Research Article

Muhammad Bilal, Shafqat Ur Rehman, Usman Younas, Alsharef Mohammad, Shahram Rezapour*, and Mustafa Inc*

Dynamical analyses and dispersive soliton solutions to the nonlinear fractional model in stratified fluids

https://doi.org/10.1515/phys-2025-0218 received February 24, 2025; accepted September 26, 2025

Abstract: This study explores the bifurcation analysis, sensitivity analysis (SA), stability analysis, and exact solitonic wave profiles for the time-fractional Benjamin-Ono (BO) equation, which models internal waves in stratified fluids, especially where dispersive effects play a significant role. These solutions are crucial for understanding ocean engineering and mathematical physics phenomena. The BO equation simulates deep-water waves, making it essential for ocean engineering applications. We employ some diverse strategies such as the new extended direct algebraic method, generalized Arnous method, and ansatz method to extract novel dispersive wave solutions. These solutions exhibit diverse shapes, such as hyperbolic, singular periodic, exponential, rational function solutions and solitary waves including dark, singular, bright, combo, and complex solutions. Our main goal is to analyze the dynamic characteristics of the model by conducting bifurcation and SA and identify the corresponding Hamiltonian function.

To ensure validity, we also conduct stability analysis using linear stability theory and outline constraint conditions. Furthermore, the bifurcation of phase portraits of ordinary differential equations corresponding to partial differential equations under investigation is also analyzed. We also demonstrate the fractional behavior of our results through visualizations (2D, 3D, contour, and density plots) by selecting suitable parametric values. Our reported results are verified using Mathematica to guarantee accuracy and validity. A detailed comparison with existing results highlights the novelty of our findings. This research contributes significantly to understand wave dynamics in nonlinear phenomena and the unique outcomes explored in this research will play a significant role in the forthcoming investigation of nonlinear problems. Moreover, the novelty of this study lies in the fact that the proposed model has not been previously explored using the aforementioned advanced methods and comprehensive dynamical analyses. This study pioneers the exploration of the fractional BO equation, yielding unique analytical results. Our techniques efficiently identify accurate solitary pulse solutions to nonlinear dynamical models with fractional parameters, making them highly successful in modeling deep-water internal waves. Our computational analytical tools are also straightforward, transparent, and reliable, reducing complexity while widening applicability. The acquired solutions are expected to have a profound impact on the study of wave propagation and related fields, offering new insights and perspectives that can inform future research and applications.

Keywords: exact wave structures, Benjamin–Ono equation, conformable operator, bifurcation analysis, sensitivity analysis, stability analysis, efficient analytical approaches

Muhammad Bilal: Department of Physics, Shanghai University, Shanghai 200444, China

Shafqat Ur Rehman: Department of Mathematics, Grand Asian University, Sialkot 51310, Pakistan

Usman Younas: Department of Mathematics, Shanghai University, Shanghai 200444, China

Alsharef Mohammad: Department of Electrical Engineering, Taif University, Al Hawiyah, Taif, Saudi Arabia

1 Introduction

In this modern technological era, engineers and scholars have been increasingly interested in obtaining exact

^{*} Corresponding author: Shahram Rezapour, Department of Medical Research, China Medical University, 40402 Taichung, Taiwan, e-mail: rezapourshahram@yahoo.ca

^{*} Corresponding author: Mustafa Inc, Department of Mathematics, Science Faculty, Firat University, 23119 Elazig, Turkey; Department of Mathematics, Saveetha School of Engineering, Saveetha Institute of Medical and Technical Sciences, Saveetha University, Chennai 602105, Tamil Nadu, India; Faculty of Informatics and Computing, Universiti Sultan Zainal Abidin, Campus Besut, 22200 Terengganu, Malaysia; Research Center of Applied Mathematics, Khazar University, Baku, Azerbaijan; Department of Computer Engineering, Biruni University, 34010 Istanbul, Turkey, e-mail: minc@firat.edu.tr

solutions to nonlinear partial differential equations (NLPDEs) using computational tools. These tools simplify complex mathematical calculations and play a key role in describing various physical systems and dynamic processes in fields such as plasma physics, fluid mechanics, hydrodynamics, quantum electronics, mathematical biology, ocean engineering, geochemistry, optical fibers, physics, and so on [1-5]. The intrinsic nonlinearity of natural phenomena has long fascinated scientists, who recognize it as a crucial element in unraveling the complexities of the universe. A plethora of physical phenomena in the universe, characterized by enigmatic behaviors, inherently involve nonlinear and dispersive components. The NLPDEs, effectively model nonlinear physical phenomena like wave propagation and instability. Mathematicians and researchers widely use these equations to study complex nonlinear wave dynamics. A dynamical system is a mathematical framework used to describe how a system evolves over time. The system's behavior is governed by differential equations, which capture its time-dependent dynamics. Dynamical systems are employed across various fields to analyze the behavior of complex systems. These fields include mathematical physics, economics, nonlinear optics, engineering, and many others.

1.1 Background and literature review

In recent years, the pursuit of analytical solutions to complex NLPDEs has emerged as a vital and captivating area of research. Notably, in the realm of soliton theory within mathematical physics, the precise solutions of NLPDEs hold paramount significance. NLPDEs serve as the fundamental tool for describing nonlinear phenomena, providing a profound understanding of their fluctuating behaviors and oscillatory mechanisms. The study of nonlinear phenomena has become particularly captivating in modern science. Consequently, there is a growing interest in utilizing efficient computational packages to secure exact solutions, thereby alleviating the complexities of algebraic computations. Various robust, efficient, and reliable analytical methods have been established in the existing literature to explore different types of solutions for nonlinear physical models [6–13].

Fractional differential equations involve derivatives of fractional order, adding complexity to the mathematical models. These equations are prominent in soliton wave theory, presenting challenges in their analysis. However, they offer a more accurate representation of real-world phenomena and

find extensive applications across nonlinear sciences. Conformable fractional operators, which maintain traditional calculus properties like Rolle's theorem and the chain rule, provide a convenient framework for comparison with existing fractional operators [14,15]. Their ease of use makes them a natural choice for practical applications and aids in understanding physical phenomena. These operators have diverse applications in different regions such as nonlinear dynamics, optical fibers, chemistry, laser optics, biology, computing networking, and engineering [16–18]. Their versatility and compatibility with established calculus principles make them valuable tools in different engineering and scientific fields.

1.2 The studied model

The Benjamin-Ono (BO) equation is a significant nonlinear model in mathematics that helps to describe one-dimensional internal waves in deep water. It was derived by two mathematicians named Benjamin [19] and Ono [20]. This partial differential equation (PDE) illustrates how onedimensional internal waves propagate across a two-layer fluid. It represents the behavior of internal waves existing in the depths of the fluid. This equation, developed by Ono and Benjamin T. Brook, is widely used in fluid dynamics and mathematical physics to study wave interactions, the evolution of wave behaviors, and wave breaking. The BO equation [20], which looks like the Korteweg-de Vries equation, was stated to elucidate internal waves in stratified fluids. It has also been applied to simulate surface wave propagation on a thinly layered structure [21], using a surface acoustic wave delay line to launch the waves. The BO equation plays a crucial role in understanding various phenomena related to internal waves [22]. In the recent past, extensive work has been done on a given model. Li [23] retrieved solutions through the trial equation method. Taghizadeh et al. [24] found exact traveling solutions with the aid of the homogeneous balance method. Kaplan et al. [25] discussed accurate solutions and conservation laws via $\exp(-\Phi(\xi))$ -expansion method and multiplier approach. Zhen et al. [26] attained different kinds of exact solutions by employing an improved projective Riccati equation technique. This study focuses on the conformable time fractional Benjamin-Ono (FBO) equation [27].

$$D_t^{2\alpha}\Theta + \beta D_x^2(\Theta^2) + \gamma D_x^4\Theta = 0, \quad 0 < \alpha \le 1,$$
 (1)

where D represents the derivative and D_t^{2a} represents twice conformable fractional derivative of function $\Theta(x,t)$ w.r.t t, while β and γ are non-zero constants.

1.3 Research aim and gap of the study

In this article, our main aim is to explore time fractional (1+1)-dimensional BO equation analytically to obtain single and combined forms of complex wave solutions of the governing model under specified parametric circumstances by the new extended direct algebraic method (NEDAM), generalized Arnous method (GAM), and ansatz method [28-30], respectively. A comprehensive review of existing literature on the BO equation reveals a significant knowledge gap: the NEDAM, GAM, and ansatz methods have not been previously utilized, and dynamical perspective of sensitivity, bifurcation, and stability analyses remains unexplored. This notable oversight underscores the importance of our research, which aims to bridge this gap by applying these innovative methods to derive novel wave structures and qualitative analyses, thereby enriching our understanding of the BO equation and its dynamics. Our current motivation is on leveraging these advanced methods to systematically investigate different classes of solutions. Furthermore, we have established a framework to efficiently categorize the solutions acquired from these innovative techniques. The methodologies employed in this study offer a significant advantage over existing methods, as they yield additional computable solutions with extra free parameters. The selection of the NEDAM, GAM, and ansatz method over conventional approaches such as the variational iteration method (VIM), Adomian decomposition method (ADM), and Hirota bilinear method (HBM) lacks a comprehensive comparative discussion in many studies. Unlike VIM and ADM, which rely on iterative corrections and series expansions, these algebraic methods offer a more direct route to exact solutions without requiring approximations or decompositions. Compared to HBM, which is limited to integrable equations and requires bilinear transformations, NEDAM, GAM, and the ansatz method apply to a broader class of nonlinear differential equations. Their primary advantage lies in their efficiency and ability to generate closed-form solutions, making them particularly useful for soliton, periodic, and rational wave solutions. However, they are limited by their reliance on correctly assuming the solution structure, a challenge not faced by iterative methods that refine approximations progressively. Additionally, while VIM and ADM provide error estimates and convergence guarantees, these algebraic methods lack inherent mechanisms to assess accuracy or stability. Despite these limitations, their ability to produce exact analytical solutions makes them valuable for exploring the fundamental properties of nonlinear evolution equations, especially in mathematical physics. Notably, many previously obtained solutions in the literature can be derived as special cases using these approaches, and importantly, new solutions are also obtained. The recommended computational methods are characterized by their simplicity, clarity, consistency, and reduced computational complexity, making them widely applicable. Furthermore, these approaches facilitate the discovery of novel results, furnishing a comprehensive framework for systematically organizing and consolidating these findings.

1.4 Structure of the study

The article is organized as follows: Conformable fractional derivative with its features is given in Section 2. Extraction of diverse traveling wave solutions is given in Section 3. In Section 4, we will discuss the sensitivity analysis (SA) of the dynamical model. Section 5 deals with bifurcation analysis. In Section 6, stability analysis is examined. In Section 7, results and discussion are represented. In Section 8, the concluding remarks are revealed.

2 Conformable derivative and its properties

The widespread applications of conformable derivatives highlight the need for more accurate mathematical methods when addressing real-world phenomena. Researchers have been exploring the behavior of nonlinear fractional partial differential equations (FPDEs) using innovative forms of fractional calculus operators like the Riemann-Liouville, Caputo-Fabrizio, and the Beta derivative. These models play a crucial role in engineering and applied sciences, offering solutions to complex problems. This particular class of derivatives offers a potent tool for scholars and practitioners to elucidate and examine a diverse range of physical, biological, and engineering systems. Among these models, the conformable fractional derivative is notable for its proficiency to reveal the core of the basic phenomenon.

• **Definition**: Suppose $g:(0,\infty)\to\mathbb{R}$ is a function. The conformable derivative of g with order α [31,32] is expressed as

$$D_t^{\alpha}g(t) = \lim_{x \to 0} \frac{g(t + xt^{1-\alpha}) - g(t)}{x}, \ \forall t > 0 \ \text{and} \ 0 < \alpha \le 1.$$

Furthermore, if g is α -differentiable in some interval $(0, \zeta)$ where $\zeta > 0$, and $\lim_{t\to 0} g_t^a(t)$ exists, we define $g_t^a(0) =$ $\lim_{t\to 0^+} g_t^{\alpha}(t)$. Some features are presented as follows.

Lemma 1. If g_1 and g_2 are α -conformable differentiables for all t > 0 and let $\alpha \in (0, 1]$.

- (i) $\mathcal{D}_t^{\alpha}(b_1g_1 + b_2g_2) = b_1\mathcal{D}_t^{\alpha}(g_1) + b_2\mathcal{D}_t^{\alpha}(g_2), \forall b_1, b_2 \in \mathbb{R}$.
- (ii) $\mathcal{D}_t^{\alpha}(t^q) = qt^{q-\alpha}, \forall q \in \mathbb{R}$.
- (iii) $\mathcal{D}_t^{\alpha}(\zeta) = 0$, where $g(t) = \zeta$ denotes a constant.
- $(iv) \ \mathcal{D}_t^\alpha(g_1g_2) = g_1\mathcal{D}_\alpha(g_2) + g_2\mathcal{D}_\alpha(g_1).$
- $(v) \ \mathcal{D}_t^a(\frac{g_1}{g_2}) = \tfrac{g_2\mathcal{D}_t^a(g_1) g_1\mathcal{D}_t^a(g_2)}{g_2^2}, \ provided \ g_2 \neq 0.$
- (vi) If g_1 is a differentiable function then $\mathcal{D}_t^a(g_1)(t)=t^{1-a}\frac{\partial g_1}{\partial t}$.

The choice of the conformable derivative over Caputo or Riemann-Liouville derivatives reflects a trade-off between capturing memory effects and ensuring analytical tractability. While Caputo and Riemann-Liouville formulations inherently model memory through non-local integral operators, their complexity often complicates analytical solutions, numerical implementation, and physical interpretation. The conformable derivative, though lacking explicit memory representation, offers a local, Leibniz-like structure that simplifies computations, preserves classical calculus rules, and facilitates explicit solutions - advantages critical for modeling systems where memory effects are secondary to simplicity, interpretability, or real time applicability. This prioritization of tractability makes conformable derivatives pragmatic for applications where approximate or efficient modeling suffices. The conformable derivative is a type of fractional derivative proposed to maintain compatibility with classical calculus, particularly the limit definition. It offers a physically meaningful way to explain memory and hereditary features in intricate systems. Its simplicity and local nature make it suitable for modeling timedependent processes in physics and engineering problems.

3 Diversity of traveling wave solutions

In this section, we utilize different techniques to earn some soliton solutions of the studied model. Prior to extracting the results we present some characteristics and weakness of the aforementioned mathematical techniques.

The NEDAM is a powerful analytical technique for obtaining exact solutions of nonlinear evolution equations, especially soliton and periodic wave solutions. It extends traditional direct algebraic approaches by incorporating more general ansatz functions and higher-degree polynomials, allowing for a wider variety of solution forms. This method is valued for its systematic structure, applicability to diverse nonlinear PDEs, and ability to generate multiple types of exact solutions, including dark, bright, combine,

and rational-type structures. However, it may become computationally intensive for complex equations due to the algebraic system's size and complexity.

The GAM refines and extends classical ansatz-based techniques by incorporating hyperbolic and trigonometric function expansions to construct more general analytical solutions. It is particularly effective in generating traveling wave solutions and is simpler in structure, often reducing the PDE to an ordinary differential equation *via* wave transformation before solving. This method is appreciated for its simplicity, versatility, and relatively low computational burden, but it can be limited in scope, often failing to capture more complex or nonstandard wave structures that the extended direct algebraic method can handle.

3.1 Application of NEDAM

The NEDAM generates a wide variety of exact solutions for nonlinear PDEs, offering flexibility and precision. It is applicable to diverse physical problems and reduces computational complexity. However, this technique has a limitation: it is ineffective when the highest derivative terms do not uniformly balance with nonlinear terms. To solve the above system by utilizing NEDAM, we use traveling wave transformation $\Theta(x,t)=Q(\eta)$, where $\eta=kx+\frac{\vartheta}{\alpha}t^{\alpha}$. Substituting this transformation in Eq. (1), after twice integration with constants of integration equal to zero, we obtain

$$yk^4O''(n) + \beta k^2O(n)^2 + \vartheta^2O(n) = 0.$$
 (2)

By applying the balance principle to Eq. (2) and equating the powers of $Q(\eta)^2$ and $Q''(\eta)$, we obtain n=2. Thus, Eq. (2) has the following form of solution:

$$Q(\eta) = b_0 + \sum_{k=1}^{n} b_k Y^k(\eta).$$
 (3)

$$O(n) = b_0 + b_1 Y(n) + b_2 Y^2(n). \tag{4}$$

By substituting Eq. (4) and its derivatives $(Y'(\eta) = \ln(B)(\mu + \lambda Y(\eta) + \nu Y^2(\eta)), B \neq 0, 1)$, in Eq. (2), and through the utilization of symbolic computer algebra software, Mathematica, we meticulously equate coefficients of similar powers of $Y(\eta)$ to zero, facilitating the identification and correlation of stable exact solutions to Eq. (1). This rigorous process ensures the comprehensive establishment of the solution set, thereby completing the solution establishment phase of our analysis.

Family-1.

$$\begin{cases} b_0 = \frac{\vartheta^2(k^4(\lambda^2 + 8\mu\nu) - \sqrt{k^8(\lambda^2 - 4\mu\nu)^2})}{2\beta k^2 \sqrt{k^8(\lambda^2 - 4\mu\nu)^2}}, \\ b_1 = \frac{6k^2\lambda\nu\vartheta^2}{\beta\sqrt{k^8(\lambda^2 - 4\mu\nu)^2}}, \\ b_2 = \frac{6k^2\nu^2\vartheta^2}{\beta\sqrt{k^8(\lambda^2 - 4\mu\nu)^2}}, \\ \gamma = -\frac{\vartheta^2}{\sqrt{k^8\ln^4(B)(\lambda^2 - 4\mu\nu)^2}}. \end{cases}$$

(1) For $\lambda^2 - 4\mu\nu < 0$ and $\nu \neq 0$. The trigonometric solutions

$$\Theta_1(x,t) = \left\{ -\frac{\vartheta^2 \left[3\tan \left(\frac{1}{2} \eta \sqrt{4\mu\nu - \lambda^2} \right)^2 + 3 \right]}{2\beta k^2} \right\}, \tag{5}$$

$$\Theta_2(x,t) = \left\{ -\frac{\vartheta^2 \left[3\cot_B \left(\frac{1}{2} \eta \sqrt{4\mu \nu - \lambda^2} \right)^2 + 3 \right]}{2\beta k^2} \right\}, \tag{6}$$

We construct multiple outcomes to Eq. (1) as follows.

$$\Theta_{3}(x,t) = \left\{ -\frac{\vartheta^{2}(3(\tan_{B}(\eta\sqrt{4\mu\nu - \lambda^{2}}) \pm \sqrt{pq}\sec_{B}(\eta\sqrt{4\mu\nu - \lambda^{2}}))^{2} + 3)}{2\beta k^{2}} \right\},\tag{7}$$

$$\Theta_4(x,t) = \left\{ -\frac{\vartheta^2(3(\cot_B(\eta\sqrt{4\mu\nu - \lambda^2}) \pm \sqrt{pq}\csc_B(\eta\sqrt{4\mu\nu - \lambda^2}))^2 + 3)}{2\beta k^2} \right\},\tag{8}$$

$$\Theta_5(x,t) = \left\{ -\frac{\vartheta^2 \left[3 \left[\cot_B \left(\frac{1}{4} \eta \sqrt{4\mu\nu - \lambda^2} \right) - \tan_B \left(\frac{1}{4} \eta \sqrt{4\mu\nu - \lambda^2} \right) \right]^2 + 12 \right]}{8\beta k^2} \right\}. \tag{9}$$

(2) For λ^2 – $4\mu\nu$ > 0 and $\nu\neq$ 0, some diverse wave solutions are obtained.

The dark solution is as follows:

$$\Theta_6(x,t) = \left\{ -\frac{\vartheta^2 \left[3 - 3 \tanh_B \left(\frac{1}{2} \eta \sqrt{\lambda^2 - 4\mu \nu} \right)^2 \right]}{2\beta k^2} \right\}.$$
 (10)

The singular solution is as follows:

$$\Theta_7(x,t) = \left\{ \frac{\vartheta^2 \left(3 - 3 \coth_B \left(\frac{1}{2} \eta \sqrt{\lambda^2 - 4\mu \nu} \right)^2 \right)}{2\beta k^2} \right\}. \tag{11}$$

The complex dark-bright solution is as follows:

$$\Theta_8(x,t) = \left\{ -\frac{\vartheta^2(3 - 3(\tanh_B(\eta\sqrt{\lambda^2 - 4\mu\nu}) \pm i\sqrt{pq}\operatorname{sech}_B(\eta\sqrt{\lambda^2 - 4\mu\nu}))^2)}{2\beta k^2} \right\}. \tag{12}$$

The mixed singular solution is as follows:

$$\Theta_{9}(x,t) = \left\{ -\frac{\vartheta^{2}(3 - 3(\coth_{B}(\eta\sqrt{\lambda^{2} - 4\mu\nu}) \pm \sqrt{pq}\operatorname{csch}_{B}(\eta\sqrt{\lambda^{2} - 4\mu\nu}))^{2})}{2\beta k^{2}} \right\}. \tag{13}$$

The dark-singular solution is as follows:

$$\Theta_{10}(x,t) = \left\{ -\frac{\vartheta^2 \left[12 - 3 \left[\coth_B \left(\frac{1}{4} \eta \sqrt{\lambda^2 - 4\mu \nu} \right) + \tanh_B \left(\frac{1}{4} \eta \sqrt{\lambda^2 - 4\mu \nu} \right) \right]^2 \right]}{8\beta k^2} \right\}.$$
(14)

(3) For $\mu\nu > 0$ and $\lambda = 0$.

The periodic solutions are as follows:

$$\Theta_{11}(x,t) = \left\{ \frac{\vartheta^2 (3\tan_B (\eta \sqrt{\mu \nu})^2 + 1)}{2\beta k^2} \right\},\tag{15}$$

$$\Theta_{12}(x,t) = \left\{ \frac{\vartheta^2 (3\cot_B(\eta\sqrt{\mu\nu})^2 + 1)}{2\beta k^2} \right\}. \tag{16}$$

Now, the mixed-trigonometric solutions are as follows:

$$\Theta_{13}(x,t) = \left\{ \frac{\vartheta^2(3(\tan_B(2\eta\sqrt{\mu\nu}) \pm \sqrt{pq} \sec_B(2\eta\sqrt{\mu\nu}))^2 + 1)}{2\beta k^2} \right\}, (17)$$

$$\Theta_{14}(x,t) = \left\{ \frac{\vartheta^2 (3(\cot_B (2\eta\sqrt{\mu\nu}) \pm \sqrt{pq} \csc_B (2\eta\sqrt{\mu\nu}))^2 + 1)}{2\beta k^2} \right\}, (18)$$

$$\Theta_{15}(x,t) = \left\{ \frac{\partial^2 \left[3 \left[\cot_B \left(\frac{1}{2} \eta \sqrt{\mu \nu} \right) - \tan_B \left(\frac{1}{2} \eta \sqrt{\mu \nu} \right) \right]^2 + 4 \right]}{8\beta k^2} \right\}. (19)$$

(4) For $\mu\nu$ < 0 and λ = 0.

The hyperbolic solution is as follows:

$$\Theta_{16}(x,t) = \left\{ \frac{\vartheta^2 (1 - 3 \tanh_B (\eta \sqrt{-\mu \nu})^2)}{2\beta k^2} \right\}.$$
 (20)

The singular solution is as follows:

$$\Theta_{17}(x,t) = \left\{ \frac{\vartheta^2 (1 - 3\coth_B(\eta \sqrt{-\mu v})^2)}{2\beta k^2} \right\}. \tag{21}$$

The different types of complex wave structures are as follows:

$$\Theta_{18}(x,t) = \left\{ \frac{\vartheta^2 (1 - 3(\tanh_B(2\eta\sqrt{-\mu\nu}) \pm i\sqrt{pq}\operatorname{sech}_B(2\eta\sqrt{-\mu\nu}))^2)}{2\beta k^2} \right\},$$
(22)

$$\Theta_{19}(x, t) = \left\{ \frac{\vartheta^{2}(1 - 3(\coth_{B}(2\eta\sqrt{-\mu v}) \pm \sqrt{pq} \operatorname{csch}_{B}(2\eta\sqrt{-\mu v}))^{2})}{2\beta k^{2}\sqrt{k^{8}\mu^{2}v^{2}}} \right\}, (23)$$

$$\Theta_{20}(x, t) = \begin{cases} \frac{\vartheta^2 \left[4 - 3 \left(\coth B \left(\frac{1}{2} \eta \sqrt{-\mu \nu} \right) + \tanh B \left(\frac{1}{2} \eta \sqrt{-\mu \nu} \right) \right)^2 \right]}{8\beta k^2} \end{cases} (24)$$

(5) For $\lambda = 0$ and $\nu = \mu$.

The periodic wave solutions are as follows:

$$\Theta_{21}(x,t) = \left\{ \frac{\vartheta^2 (3\tan_B(\mu\eta)^2 + 1)}{2\beta k^2} \right\},\tag{25}$$

$$\Theta_{22}(x,t) = \left\{ \frac{\vartheta^2 (3\cot_B(\mu\eta)^2 + 1)}{2\beta k^2} \right\},\tag{26}$$

$$\Theta_{23}(x,t) = \left\{ \frac{\vartheta^2(3(\tan_B(2\mu\eta) \pm \sqrt{pq}\sec_B(2\mu\eta))^2 + 1)}{2\beta k^2} \right\}, \quad (27)$$

$$\Theta_{24}(x,t) = \left\{ \frac{\vartheta^2 (3(-\cot_B(2\mu\eta) \pm \sqrt{pq}\csc_B(2\mu\eta))^2 + 1)}{2\beta k^2} \right\}, (28)$$

$$\Theta_{25}(x,t) = \left\{ \frac{\vartheta^2 \left[3 \left(\cot g \left(\frac{\mu \eta}{2} \right) - \tan g \left(\frac{\mu \eta}{2} \right) \right]^2 + 4 \right]}{8\beta k^2} \right\}.$$
 (29)

(6) For $\lambda = 0$ and $\nu = -\mu$.

Exact wave solutions are as follows:

$$\Theta_{26}(x,t) = \left\{ \frac{3\vartheta^2(\tanh_B(\mu\eta)^2 - 1)}{2\beta k^2} \right\},\tag{30}$$

$$\Theta_{27}(x,t) = \left\{ \frac{3\vartheta^2(\coth_B(\mu\eta)^2 - 1)}{2\beta k^2} \right\},\tag{31}$$

$$\Theta_{28}(x,t) = \left\{ \frac{3\vartheta^2(-1 + (-\tanh_B(2\mu\eta) \pm i\sqrt{pq}\operatorname{sech}_B(2\mu\eta))^2)}{2\beta k^2} \right\},$$
(32)

$$\Theta_{29}(x,t) = \left\{ \frac{3\vartheta^{2}((-\coth_{B}(2\mu\eta) \pm \sqrt{pq} \operatorname{csch}_{B}(2\mu\eta))^{2} - 1)}{2\beta k^{2}} \right\},$$
(33)

$$\Theta_{30}(x,t) = \begin{cases} \frac{\partial^2 \left[3 \left[\coth_B \left(\frac{\mu \eta}{2} \right) + \tanh_B \left(\frac{\mu \eta}{2} \right) \right]^2 - 12 \right]}{8\beta k^2 \sqrt{k^8 \mu^4}} \end{cases}. (34)$$

(8) For $\mu = 0$ and $\lambda \neq 0$.

Combined-hyperbolic solutions are as follows:

$$\Theta_{31}(x,t) = \begin{cases} \frac{\vartheta^2 \left(\frac{\sqrt{k^8 \lambda^4} \left((\cosh g(\lambda \eta) - \sinh g(\lambda \eta)) \left(\cosh g(\lambda \eta) - 10p - \sinh g(\lambda \eta) \right) + p^2 \right)}{\lambda^2 \left(\cosh g(\lambda \eta) + p - \sinh g(\lambda \eta) \right)^2} - k^4 \right)}{2\beta k^6} \end{cases}, \tag{35}$$

$$\Theta_{32}(x,t) = \begin{cases} \frac{\vartheta^2 \left[\left(1 - \frac{12q(\cosh_B(\lambda \eta) + \sinh_B(\lambda \eta))}{(\cosh_B(\lambda \eta) + q + \sinh_B(\lambda \eta))^2} \right) - 1 \right]}{2\beta k^2} \end{cases}. (36)$$

(9) For $\mu = 0$, $\lambda = \gamma$ and $\nu = r\gamma$. Rational function solution is as follows:

$$\Theta_{32}(x,t) = \begin{cases} \frac{\vartheta^2 \left[\left(1 - \frac{12q(\cosh_B(\lambda\eta) + \sinh_B(\lambda\eta))}{(\cosh_B(\lambda\eta) + q + \sinh_B(\lambda\eta))^2} \right) - 1 \right]}{2\beta k^2} \\ & \varepsilon_0 = -\frac{\log^2(\delta)(\beta\sigma_2 + 4\gamma k^2)}{\beta}, \quad \varepsilon_1 = 0, \\ & \varepsilon_2 = \frac{\rho \log^2(\delta)(\beta\sigma_2 + 6\gamma k^2)}{\beta}, \quad \sigma_1 = 0, \quad \vartheta = 2\sqrt{\gamma} k^2 \log(\delta). \end{cases}$$

At $\delta = e, \rho = 4A^2$, we obtain solitary wave solution in the following form:

$$\Theta_{33}(x,t) = \left\{ \frac{\vartheta^2(k^4\chi^2(r^2(12p^2 - 12pq + q^2)B^{2\eta\chi} + p^2 + 2pr(6p - q)B^{\eta\chi}) - k^4\chi^2(p - qrB^{\eta\chi})^2}{2\beta k^2k^4\chi^2(p - qrB^{\eta\chi})^2} \right\}, \tag{37}$$

where $\eta = kx + \frac{\vartheta}{a}t^a$, for all above solutions.

3.2 Application of GAM

The GAM effectively derives exact solutions for nonlinear equations with strong nonlinearity and dispersion. It transforms equations into simpler forms, yielding explicit solutions, and adapts to various nonlinear evolution equations. However, this method has a limitation: it is ineffective when the highest derivative terms do not uniformly balance with nonlinear terms. In this section, we employ the GAM to derive solitary wave solutions to the BO equation. The GAM involves assuming a solution of the form

$$Q(\eta) = \varepsilon_0 + \sum_{k=1}^n \frac{\varepsilon_k + \sigma_k \Phi'(\eta)^k}{\Phi(\eta)^k}.$$
 (38)

For n = 2, the GAM proposes a solution to Eq. (2) in the following form:

$$Q(\eta) = \varepsilon_0 + \frac{\varepsilon_1 + \sigma_1 \Phi'(\eta)}{\Phi(\eta)} + \frac{\varepsilon_2 + \sigma_2 \Phi'(\eta)^2}{\Phi(\eta)^2}.$$
 (39)

By substituting Eq. (39) into Eq. (2) along with its derivatives $(\Phi'(\eta)^2 = (\Phi(\eta)^2 - \rho)\log^2(\delta))$, we receive a polynomial in terms of $\frac{1}{\Phi(\eta)} \frac{\Phi'(\eta)}{\Phi(\eta)}$. Collecting and equating coefficients, we obtain a system of algebraic equations, yielding two solution sets

$$\begin{split} \varepsilon_0 &= -\frac{\log^2(\delta)(\beta\sigma_2 + 4\gamma k^2)}{\beta}, \quad \varepsilon_1 = 0, \\ \varepsilon_2 &= \frac{\rho \log^2(\delta)(\beta\sigma_2 + 6\gamma k^2)}{\beta}, \quad \sigma_1 = 0, \quad \vartheta = 2\sqrt{\gamma} \, k^2 \log(\delta). \end{split}$$

and

$$\begin{split} \varepsilon_0 &= \sigma_2(-\log^2(\delta)), \quad \varepsilon_1 = 0, \\ \varepsilon_2 &= \frac{\rho \log^2(\delta)(\beta \sigma_2 + 6 \gamma k^2)}{\beta}, \quad \sigma_1 = 0, \quad \vartheta = 2i \sqrt{\gamma} \, k^2 \log(\delta). \end{split}$$

According to set-1

$$\Theta_1(x,t) = \frac{2\gamma k^2 \left[3 \operatorname{sech}^2 \left(k \left(\frac{2\sqrt{\gamma} k t^a}{a} + x \right) \right) - 2 \right]}{\beta}.$$
 (40)

According to set-2

$$\begin{split} \varepsilon_0 &= \sigma_2(-\log^2(\delta)), \quad \varepsilon_1 = 0, \\ \varepsilon_2 &= \frac{\rho \log^2(\delta)(\beta \sigma_2 + 6\gamma k^2)}{\beta}, \quad \sigma_1 = 0, \quad \vartheta = 2i\sqrt{\gamma} \, k^2 \log(\delta). \end{split}$$

At $\delta = e$, $\rho = 4A^2$, we obtain hyperbolic solution in this form

$$\Theta_2(x,t) = \frac{6\gamma k^2 \operatorname{sech}^2\left(kx + \frac{2i\sqrt{\gamma}k^2t^\alpha}{\alpha}\right)}{\beta}.$$
 (41)

3.3 Ansatz method

To construct the solutions, hyperbolic and exponential ansatz method is used in Sections 3.3.1-3.3.3

3.3.1 Solitary wave solution

For solitary wave solutions, we have

$$\Theta(x,t) = a_1 \operatorname{sech}^2 \eta + a_0, \quad \eta = kx + \frac{\vartheta}{\alpha} t^{\alpha}, \quad (42)$$

where a_0 , $a_1 \neq 0$, k, and ϑ are the arbitrary constants. Substituting Eq. (42) in Eq.(2), we secure equations in the following forms:

$$16a_{1}\gamma k^{4} - 4a_{1}^{2}\beta k^{2} - 4a_{0}a_{1}\beta k^{2} - 2a_{1}\vartheta^{2} = 0,$$

$$-136a_{1}\gamma k^{4} + 28a_{1}^{2}\beta k^{2} + 16a_{0}a_{1}\beta k^{2} + 8a_{1}\vartheta^{2} = 0,$$

$$240a_{1}\gamma k^{4} - 44a_{1}^{2}\beta k^{2} - 12a_{0}a_{1}\beta k^{2} - 6a_{1}\vartheta^{2} = 0,$$

$$20a_{1}^{2}\beta k^{2} - 120a_{1}\gamma k^{4} = 0.$$

$$(43)$$

Solving the above equations we achieve

8 — Muhammad Bilal *et al*.

$$a_0 = -\frac{4\gamma k^4 + \vartheta^2}{2\beta k^2}, \quad a_1 = \frac{6\gamma k^2}{\beta}.$$

Hence, the solitary wave solution is presented as

$$\Theta(x,t) = -\frac{4\gamma k^4 - 12\gamma k^4 \operatorname{sech}^2(kx + \frac{\vartheta}{\alpha}t^{\alpha}) + \vartheta^2}{2\beta k^2}.$$
 (44)

3.3.2 Dark wave solution

For dark wave solutions, we obtain

$$\Theta(x,t) = a_1 \tanh^2 \eta + a_0, \quad \eta = kx + \frac{\vartheta}{\alpha} t^{\alpha}, \quad (45)$$

where a_0 , $a_1 \neq 0$, k, and ϑ are the arbitrary constants. Substituting Eq. (45) in Eq. (2), we secure equations in the following forms:

$$-16a_{1}\gamma k^{4} + 4a_{0}a_{1}\beta k^{2} + 2a_{1}\vartheta^{2} = 0,$$

$$136a_{1}\gamma k^{4} + 12a_{1}^{2}\beta k^{2} - 16a_{0}a_{1}\beta k^{2} - 8a_{1}\vartheta^{2} = 0$$

$$-240a_{1}\gamma k^{4} - 32a_{1}^{2}\beta k^{2} + 12a_{0}a_{1}\beta k^{2} + 6a_{1}\vartheta^{2} = 0,$$

$$120a_{1}\gamma k^{4} + 20a_{1}^{2}\beta k^{2} = 0.$$
(46)

Solving the above system we achieve

$$a_0 = \frac{\vartheta^2 - 8\gamma k^4}{2\beta k^2}, \quad a_1 = -\frac{6\gamma k^2}{\beta}.$$

Hence, the dark wave solution is presented as

$$\Theta(x,t) = -\frac{-8\gamma k^4 + 12\gamma k^4 \tanh^2(kx + \frac{\vartheta}{\alpha}t^{\alpha}) + \vartheta^2}{2\beta k^2}.$$
 (47)

3.3.3 Exponential solution

For exponential solution, we have

$$\Theta(x,t) = \frac{a_2 \exp \eta}{(\exp \eta + 1)^2} + a_1, \quad \eta = kx + \frac{\vartheta}{\alpha} t^{\alpha}, \quad (48)$$

where a_0 , $a_1 \neq 0$, k, and ϑ are the arbitrary constants. Substituting Eq. (48) in Eq. (2), we secure equations in the following forms:

$$a_{2}yk^{4} + 2a_{1}a_{2}\beta k^{2} + a_{2}\vartheta^{2} = 0,$$

$$a_{2}yk^{4} + 2a_{1}a_{2}\beta k^{2} + a_{2}\vartheta^{2} = 0,$$

$$66a_{2}yk^{4} - 12a_{2}^{2}\beta k^{2} - 12a_{1}a_{2}\beta k^{2} - 6a_{2}\vartheta^{2} = 0,$$

$$-26a_{2}yk^{4} + 4a_{2}^{2}\beta k^{2} - 4a_{1}a_{2}\beta k^{2} - 2a_{2}\vartheta^{2} = 0,$$

$$-26a_{2}yk^{4} + 4a_{2}^{2}\beta k^{2} - 4a_{1}a_{2}\beta k^{2} - 2a_{2}\vartheta^{2} = 0.$$

$$(49)$$

Solving the above system we achieve

$$a_1 = -\frac{\gamma k^4 + \vartheta^2}{2\beta k^2}, a_2 = \frac{6\gamma k^2}{\beta}.$$

Hence, the exponential solution is presented as

$$\Theta(x,t) = -\frac{\gamma k^2}{2\beta} - \frac{\vartheta^2}{2\beta k^2} + \frac{3\gamma k^2}{\beta \left(\frac{1}{2} \left(e^{-kx - \frac{\vartheta}{\alpha}t^{\alpha}} + e^{kx + \frac{\vartheta}{\alpha}t^{\alpha}}\right) + 1\right)}.$$
(50)

4 SA

This section explores the SA of the governing model. SA [33,34] of dynamical models offers valuable insights into system behavior, supports model validation and calibration, aids in risk assessment and management, guides optimization and control strategies, and contributes to uncertainty quantification. Our approach investigates the effects of small perturbations in initial conditions on the system's dynamics. We analyze Eq. (2) and transform it into a dynamical system

$$\frac{\mathrm{d}Q}{\mathrm{d}\eta} = \mathcal{H}(\eta),$$

$$\frac{\mathrm{d}\mathcal{H}}{\mathrm{d}\eta} = -p_1 Q(\eta)^2 - p_2 Q(\eta),$$
(51)

where $p_1 = \frac{\beta}{\gamma \kappa^2}$ and $p_2 = \frac{\vartheta^2}{\gamma \kappa^4}$. The two solution curves are formulated, which are manifested in Figures 1–4, using different parameter values $\vartheta = 0.4$, $\beta = 0.5$, $\kappa = 0.6$, $\gamma = 0.7$. Figure 1 displays the two solutions with initial conditions $(Q, \mathcal{H}) = (0, 0)$ in blue curve (solid) and $(Q, \mathcal{H}) = (0, 0.05)$ in yellow curve (dash). Figure 2 exemplifies the two solutions with initial conditions $(Q, \mathcal{H}) = (0, 0)$ in blue curve (solid) and $(Q, \mathcal{H}) = (0.08, 0.09)$ in yellow curve (dash). Figure 3 discloses the two solutions with initial conditions $(Q, \mathcal{H}) = (0, 0)$ in

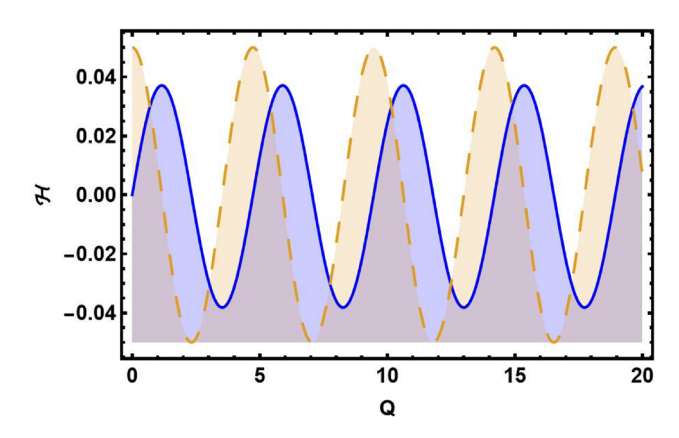


Figure 1: Graphical visualization of SA for Eq. (51) with initial conditions $(Q, \mathcal{H}) = (0, 0)$ in blue curve (solid) and $(Q, \mathcal{H}) = (0, 0.05)$ in yellow curve (dash).

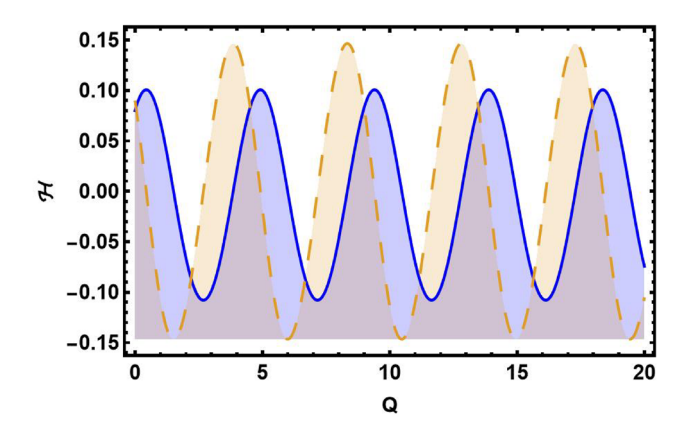


Figure 2: Graphical visualization of SA for Eq. (51) with initial conditions $(Q, \mathcal{H}) = (0, 0)$ in blue curve (solid) and $(Q, \mathcal{H}) = (0.08, 0.09)$ in yellow curve (dash).

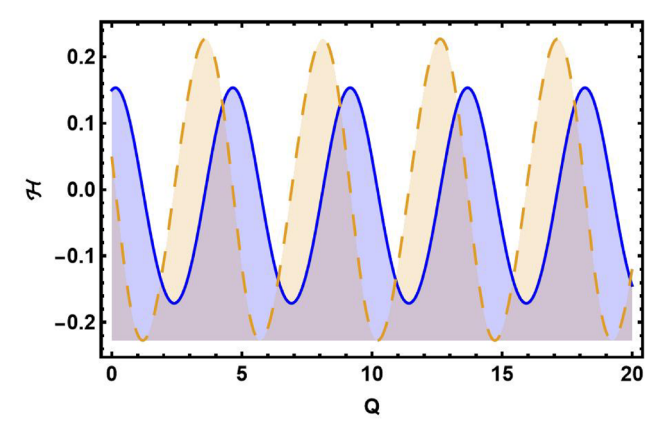


Figure 3: Graphical visualization of SA for Eq. (51) with initial conditions $(Q, \mathcal{H}) = (0, 0)$ in blue curve (solid) and $(Q, \mathcal{H}) = (0.15, 0.05)$ in yellow curve (dash).

blue curve (solid) and (Q, \mathcal{H}) = (0.15, 0.05) in yellow curve (dash). Figure 4 personifies the two solutions with initial

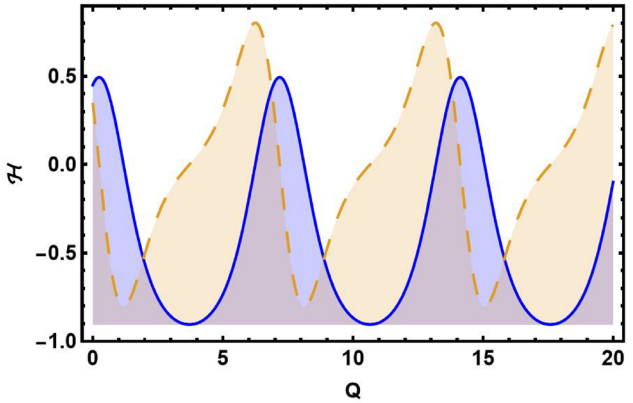


Figure 4: Graphical visualization of SA for Eq. (51) with initial conditions $(Q, \mathcal{H}) = (0, 0)$ in blue curve (solid) and $(Q, \mathcal{H}) = (0.45, 0.35)$ in yellow curve (dash).

conditions $(Q, \mathcal{H}) = (0, 0)$ in blue curve (solid) and as $(Q, \mathcal{H}) = (0.45, 0.35)$ in yellow curve (dash). The figures show that a minor adjustment in the initial conditions leads to a substantial difference in the resulting solution, indicating that the model exhibits high sensitivity. SA is an essential technique for comprehending complex systems and making informed decisions across various fields of nonlinear science.

5 Bifurcation analysis

The primary objective of bifurcation analysis is to comprehend how the qualitative behavior of a dynamical system evolves as a parameter is varied. A bifurcation occurs when such variations induce substantial changes in the system, giving rise to new dynamic behaviors. As the parameter shifts, equilibrium points, periodic patterns, or other

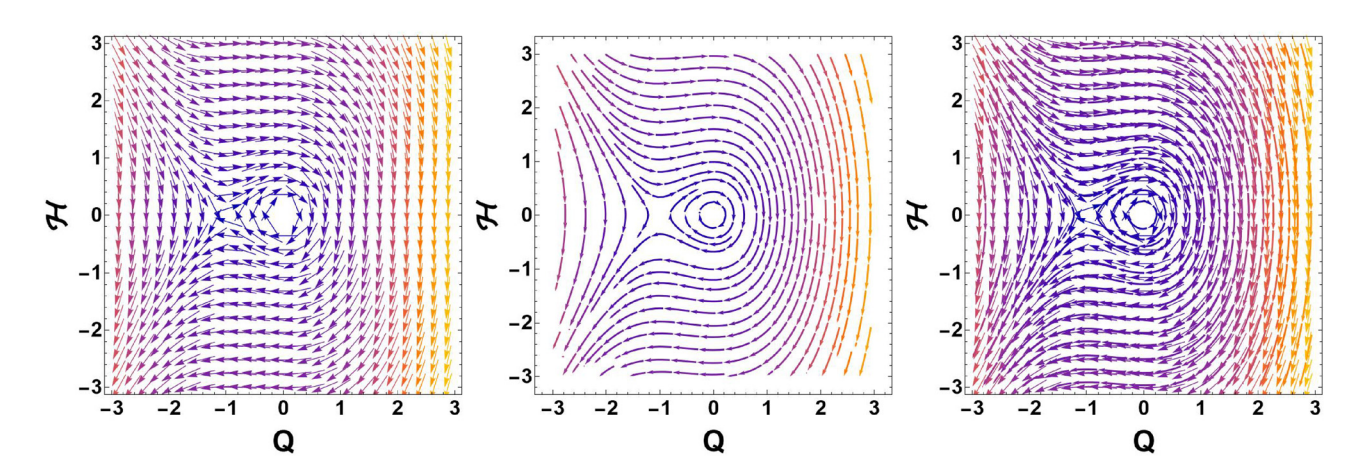


Figure 5: $p_1 > 0$ and $p_2 > 0$.

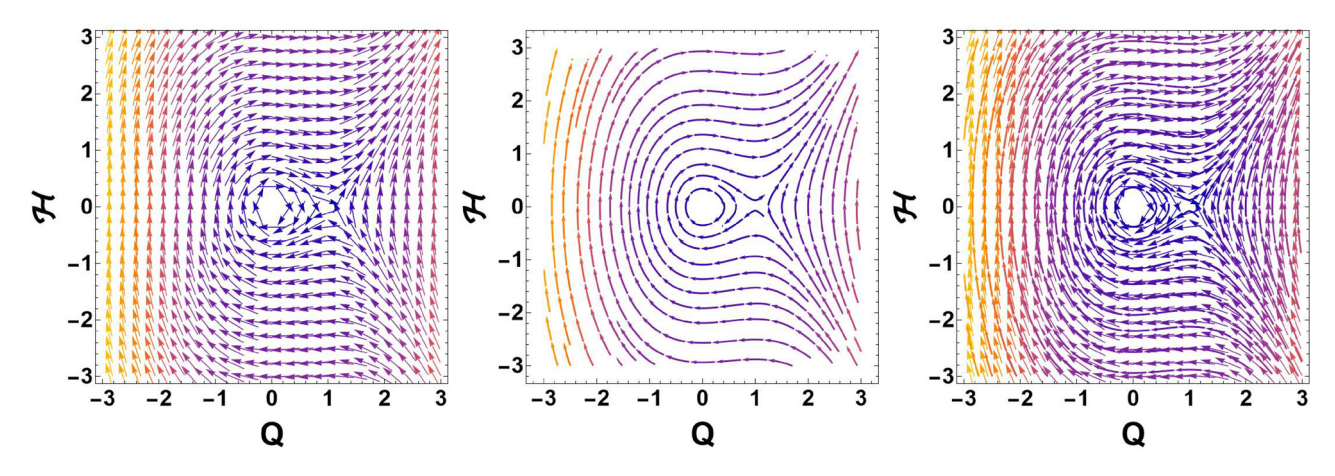


Figure 6: $p_1 < 0$ and $p_2 > 0$.

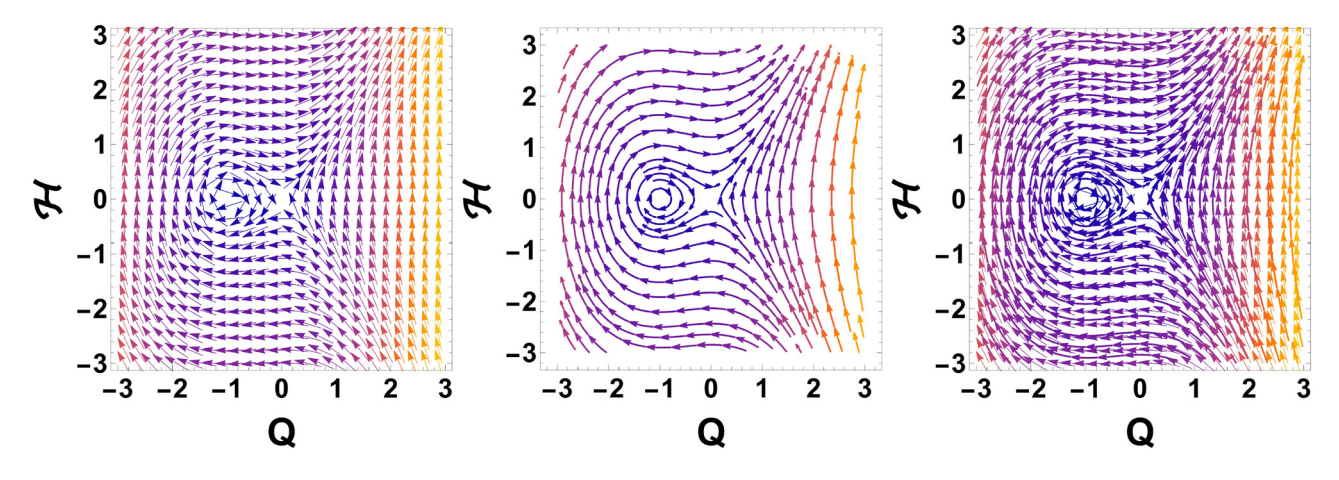


Figure 7: $p_1 < 0$ and $p_2 < 0$.

system features may emerge, vanish, or experience changes in stability [35–37]. Using bifurcation theory, we shall analyze Eq. (1) in this section. It is possible to examine governing equation as a planar dynamical system by applying a Galilean transformation.

$$\begin{cases} \frac{\mathrm{d}Q}{\mathrm{d}\eta} = \mathcal{H}(\eta), \\ \frac{\mathrm{d}\mathcal{H}}{\mathrm{d}\eta} = -p_1 Q(\eta)^2 - p_2 Q(\eta). \end{cases}$$
 (52)

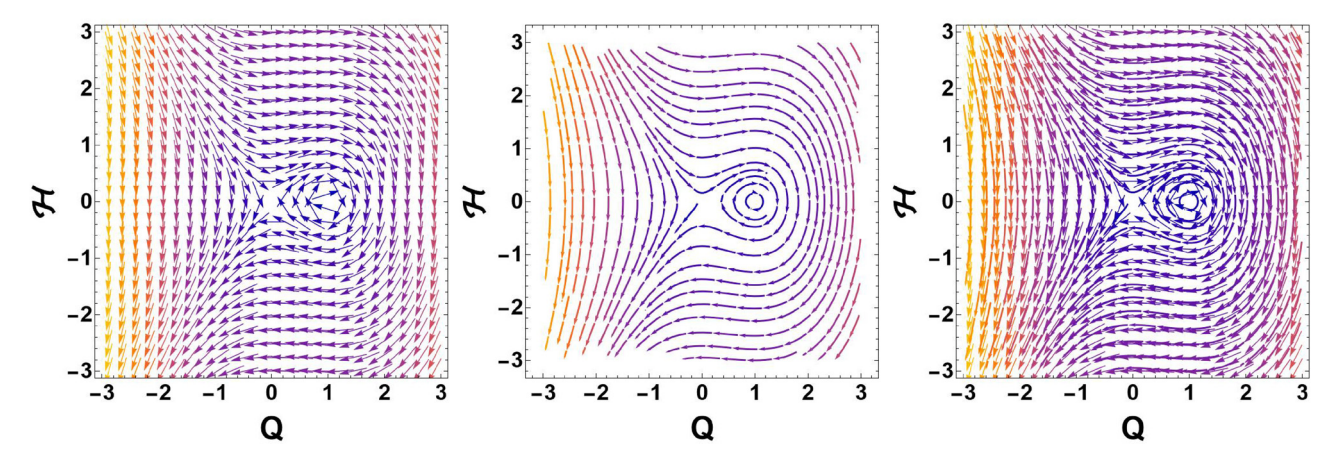


Figure 8: $p_1 > 0$ and $p_2 < 0$.

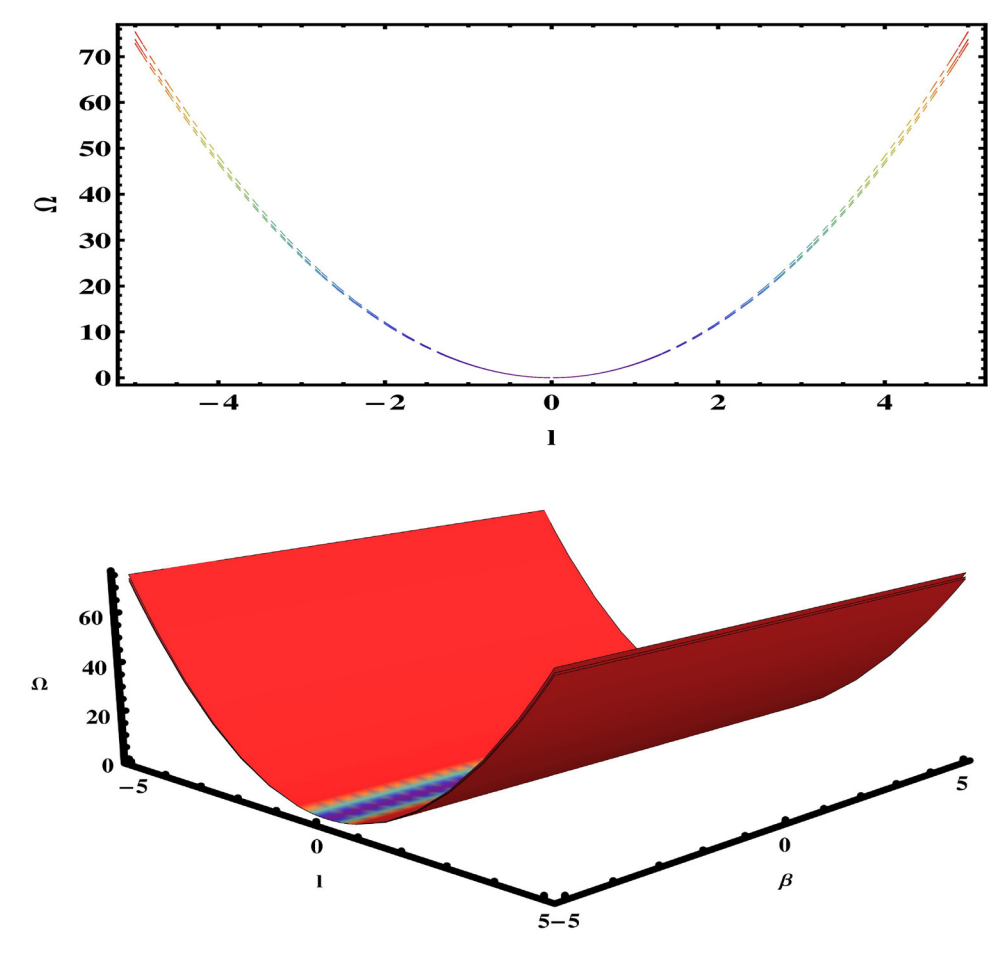


Figure 9: The dispersion relation between frequency Ω and wave number l of Eq. (60) with the suitable choice of parametric values $y = \{8.5, 9.1, 8.7\}$; $q_0 = 0.001$; $\beta = \{3.7, 2.5, 4.8\}$.

The Hamiltonian function for Eq. (52) is

$$\mathcal{T}(Q,\mathcal{H}) = \frac{\mathcal{H}^2}{2} + p_1 \frac{Q^3}{3} + p_2 \frac{Q^2}{2}.$$
 (53)

The Hamiltonian function plays a crucial role in governing the dynamics of a system by representing its total energy, typically comprising kinetic and potential components. In conservative systems, where the Hamiltonian is time-independent, it acts as a conserved quantity, ensuring energy preservation and constraining phase-space trajectories. This conservation property directly influences stability, equilibrium behavior, and integrability, as systems with a well-defined Hamiltonian often exhibit structured dynamics, such as periodic or quasi-periodic motion. Moreover, in canonical Hamiltonian systems, Poisson brackets govern evolution, ensuring symplectic structure preservation and enabling the application of powerful analytical techniques like Liouville's theorem and integrability analysis. When the Hamiltonian structure is perturbed or

non-existent, dissipative effects arise, leading to energy dissipation and potentially chaotic behavior, highlighting its fundamental role in differentiating between stable and non-conservative dynamics. To solve system (52), the system (52) has two equilibrium points, which are listed below:

 w_1 = (0,0), w_2 = ($-\frac{p_2}{p_1}$, 0). For system (52), the Jacobian matrix determinant is

$$D(Q, \mathcal{H}) = \begin{vmatrix} 0 & 1 \\ -2p_1Q - p_2 & 0 \end{vmatrix} = 2p_1Q + p_2.$$
 (54)

We know that

- If $D(Q, \mathcal{H}) < 0$, then (Q, \mathcal{H}) is a saddle.
- If $D(Q, \mathcal{H}) > 0$, then (Q, \mathcal{H}) is a center.
- If $D(Q, \mathcal{H}) = 0$, then (Q, \mathcal{H}) is a cuspidal.

The results that may be achieved by varying the relevant parameter are listed below. 12 — Muhammad Bilal et al. DE GRUYTER

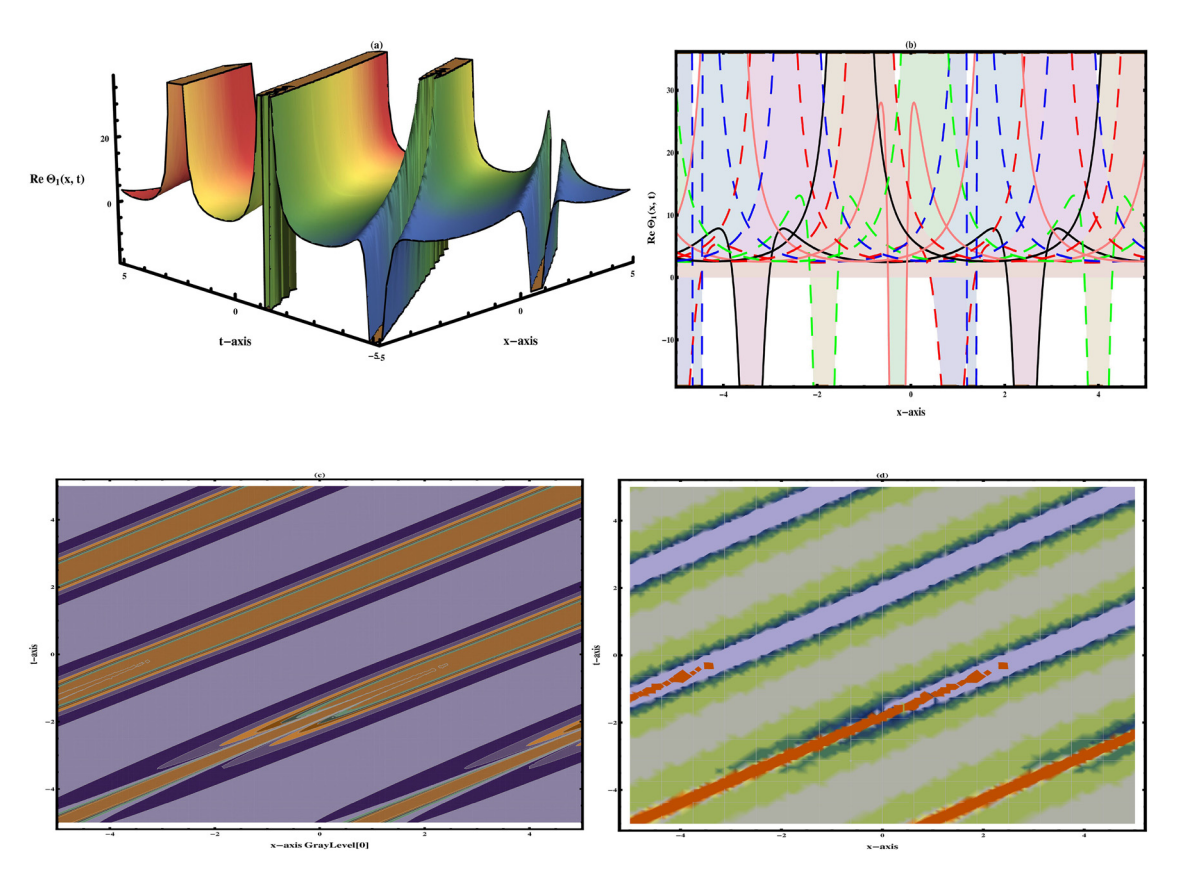


Figure 10: Visualization of Eq. (5) reveals the periodic wave structure under different arbitrary values k = 0.5, $\lambda = 0.7$, $\mu = 0.75$, $\beta = -1.5$, $\vartheta = 0.8$, $\nu = 1.7$, and B = e, at $\alpha = 0.98$.

Case-1: When $p_1 > 0$ and $p_2 > 0$.

By picking certain values for the parameters $\kappa = 2$, $\vartheta = 4$, $\gamma = 1$, $\beta = 4$, we note that (0, 0) is center whereas (–1, 0) is the saddle, which is illustrated in Figure 5.

Case-2: When
$$p_1 < 0$$
 and $p_2 > 0$.

By setting the parameters $\kappa = 2$, $\vartheta = 4$, $\gamma = 1$, $\beta = -4$, we identify that (0, 0) and (1, 0) are two equilibrium points (Eqps), in which (0, 0) behaves as a center point, as clarified in Figure 6. Moreover, (1, 0) behaves as saddle point.

Case-3: When $p_1 < 0$ and $p_2 < 0$.

By taking the parameters $\kappa = 2$, $\vartheta = 4$, $\gamma = -1$, $\beta = 4$, we identify that w_1 behaves as saddle point, whereas w_2 is obviously the center point in this case as elucidated in Figure 7.

Case-4: When $p_1 > 0$ and $p_2 < 0$.

By choosing the parameters $\kappa = 2$, $\vartheta = 4$, $\gamma = -1$, $\beta = -4$, we identify that (0, 0) and (1, 0), and are two Eqps, in which (0, 0) behaves as a saddle point, whereas (1, 0) behaves as center point as elucidated in Figure 8.

6 Stability analysis

For stability assessment, we utilize the concept of standard linear stability analysis [38] and here assume α = 1 in Eq. (1). The hypothesis for Eq. (1) is as follows:

$$\Theta(x,t) = \mu W(x,t) + q_0, \tag{55}$$

where q_0 is the steady state solution for Eq. (1). Steady state solution is used in stability analysis because it simplifies the system via linearization and spectral methods, represents physically meaningful equilibria, enables predictive insights into long-term behavior, and serves as benchmarks for bifurcations and phase transitions. For systems without steady states, stability is analyzed using alternative frameworks like Poincaré maps or Lyapunov exponents. However, steady states remain foundational due to their simplicity and interpretability. Substituting Eq. (55) in Eq. (1), we obtain

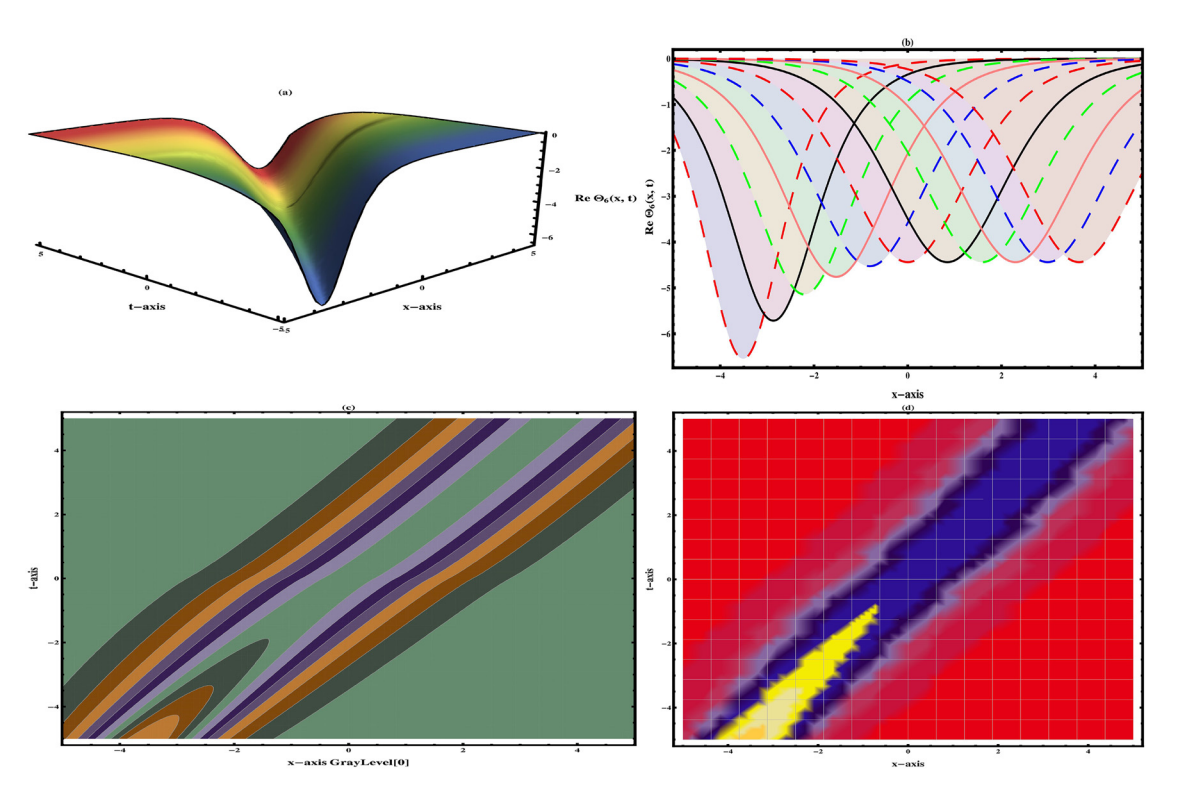


Figure 11: Visualization of Eq. (10) displays the dark wave structure under different arbitrary values k = 0.65, $\beta = 2$, $\lambda = 1.1$, $\mu = -0.75$, $\vartheta = 0.5$, $\nu = 0.7$, and B = e, at $\alpha = 0.91$.

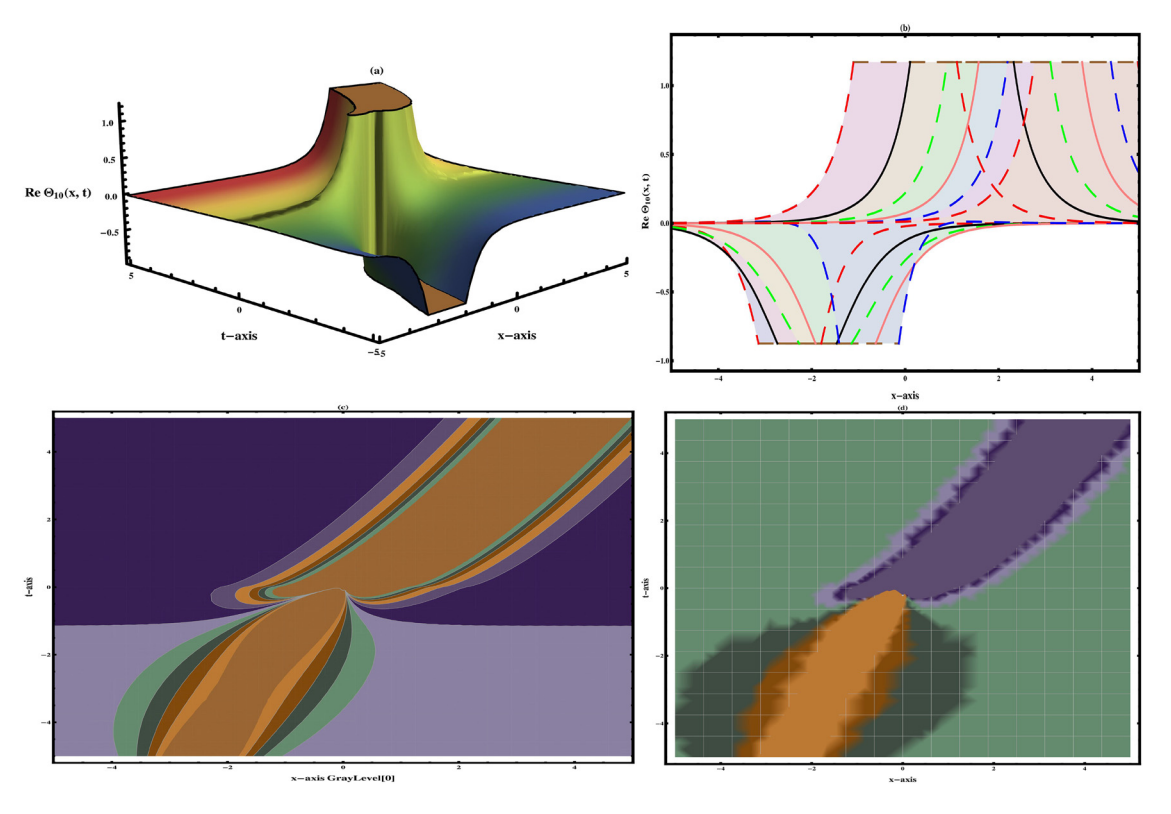


Figure 12: Visualization of Eq. (14) exhibits the dark-singular wave structure under different arbitrary values k = 0.8, $\lambda = 0.7$, $\mu = -0.65$, $\beta = 1.1$, ϑ = 0.7, ν = 1.2, and B = e, at α = 0.72.

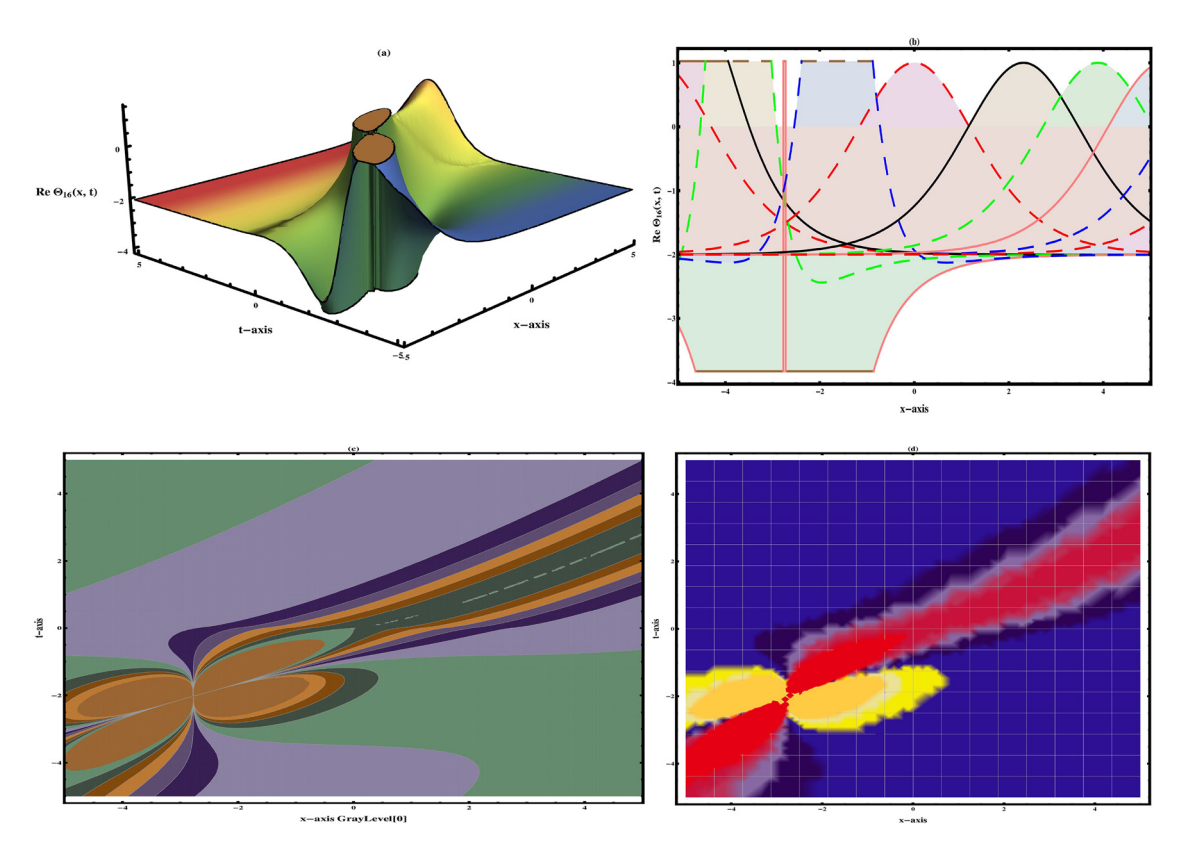


Figure 13: Visualization of Eq. (20) exhibits the hyperbolic wave structure under different arbitrary values k = 0.75, $\lambda = 1.4$, $\mu = -0.95$, $\beta = -1.5$, $\vartheta = 1.3$, $\nu = 0.6$, and B = e, at $\alpha = 0.75$.

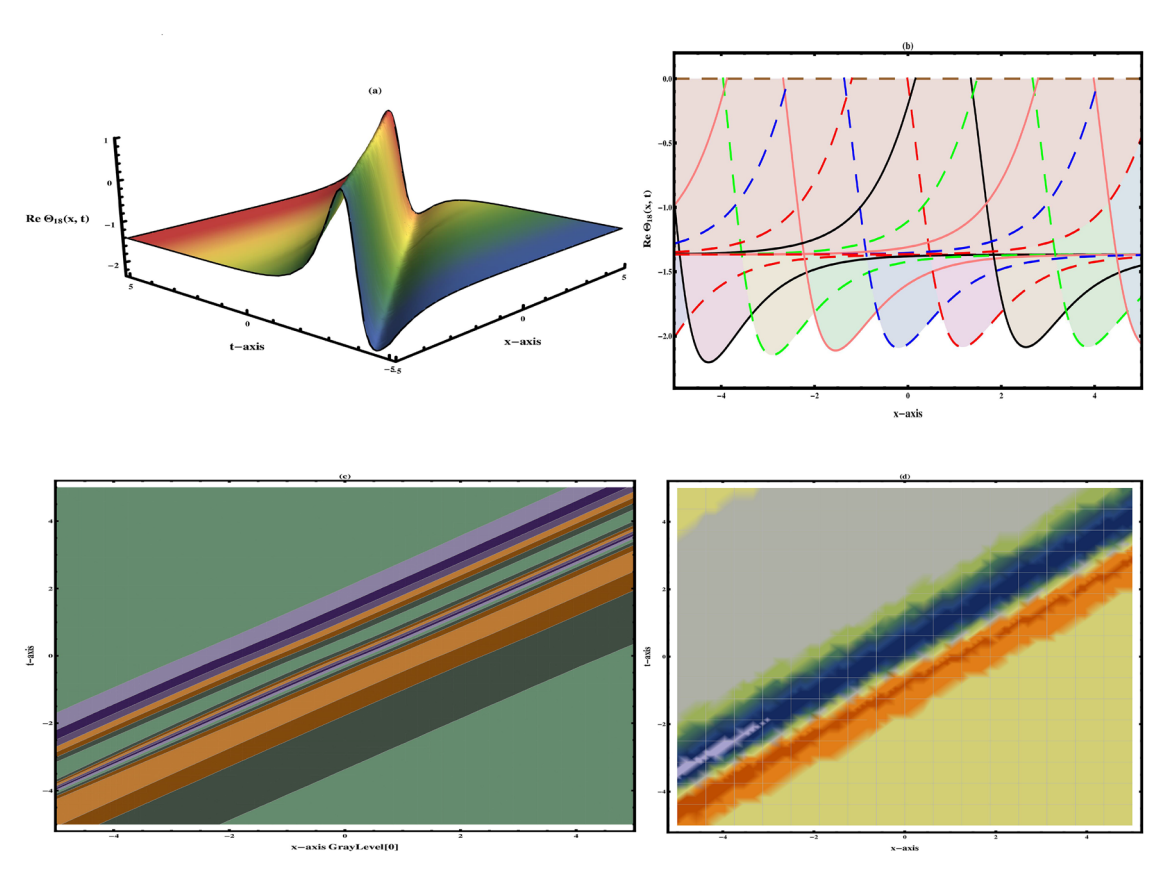


Figure 14: Visualization of Eq. (22) shows the bright-dark wave structure under different arbitrary values $p=0.7, \nu=0.9, \lambda=0.7, \mu=-0.95, q=0.5, k=0.6, \beta=1.3, \vartheta=0.8,$ and B=e, at $\alpha=0.98$.

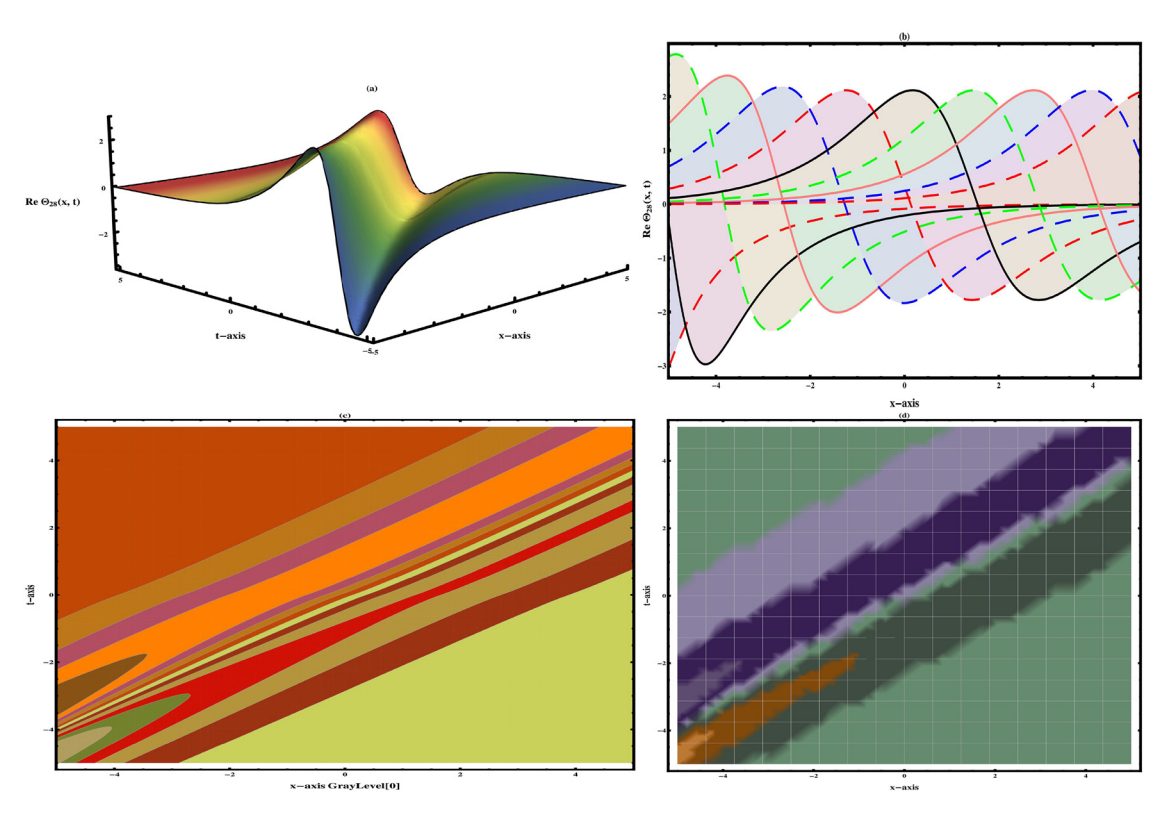


Figure 15: Visualization of Eq. (32) exhibits the bright-dark wave structure under different arbitrary values p=1.7, $\beta=1.5$, $\vartheta=0.8$, $\mu=0.55$, q=0.7, k=0.6, and B=e, at $\alpha=0.94$.

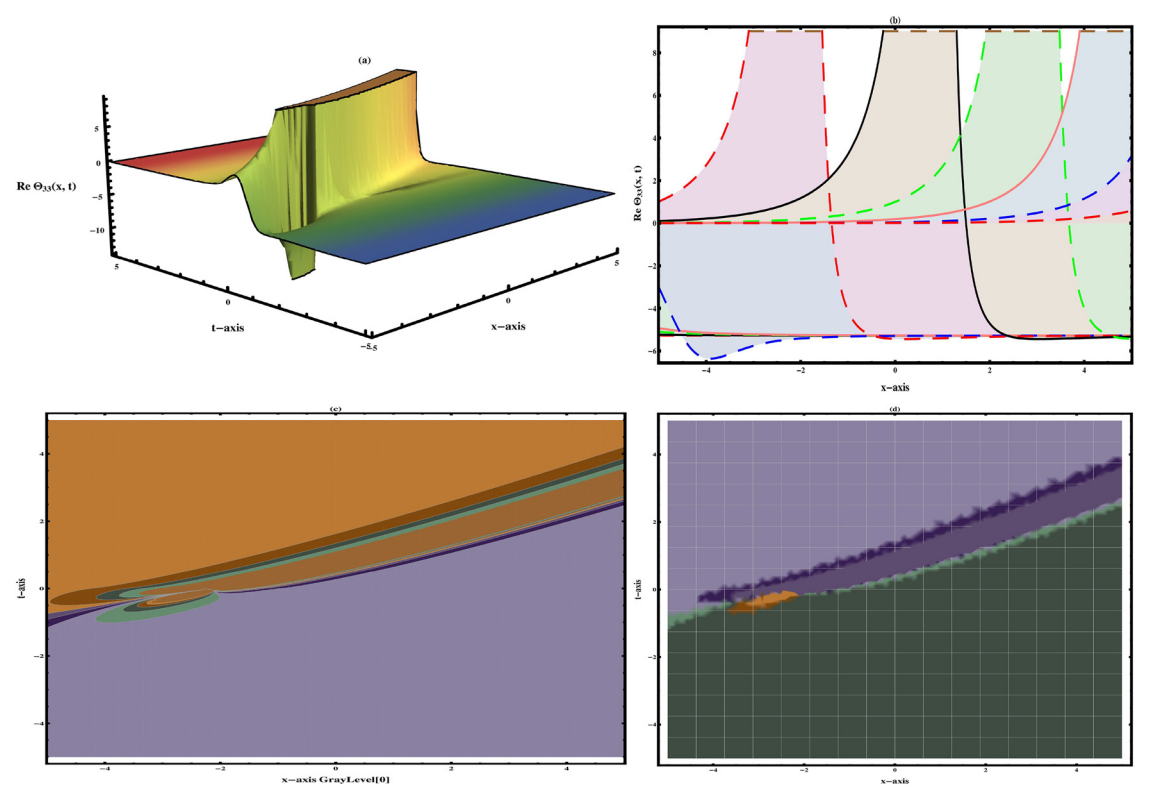


Figure 16: Visualization of Eq. (37) shows the plane wave under different arbitrary values p = 0.7, q = 1.7, k = 0.6, r = 2, $\lambda = 2.4$, $\chi = 1.3$, $\beta = 1.5$, $\vartheta = 1.4$, and B = e, at $\alpha = 0.82$.

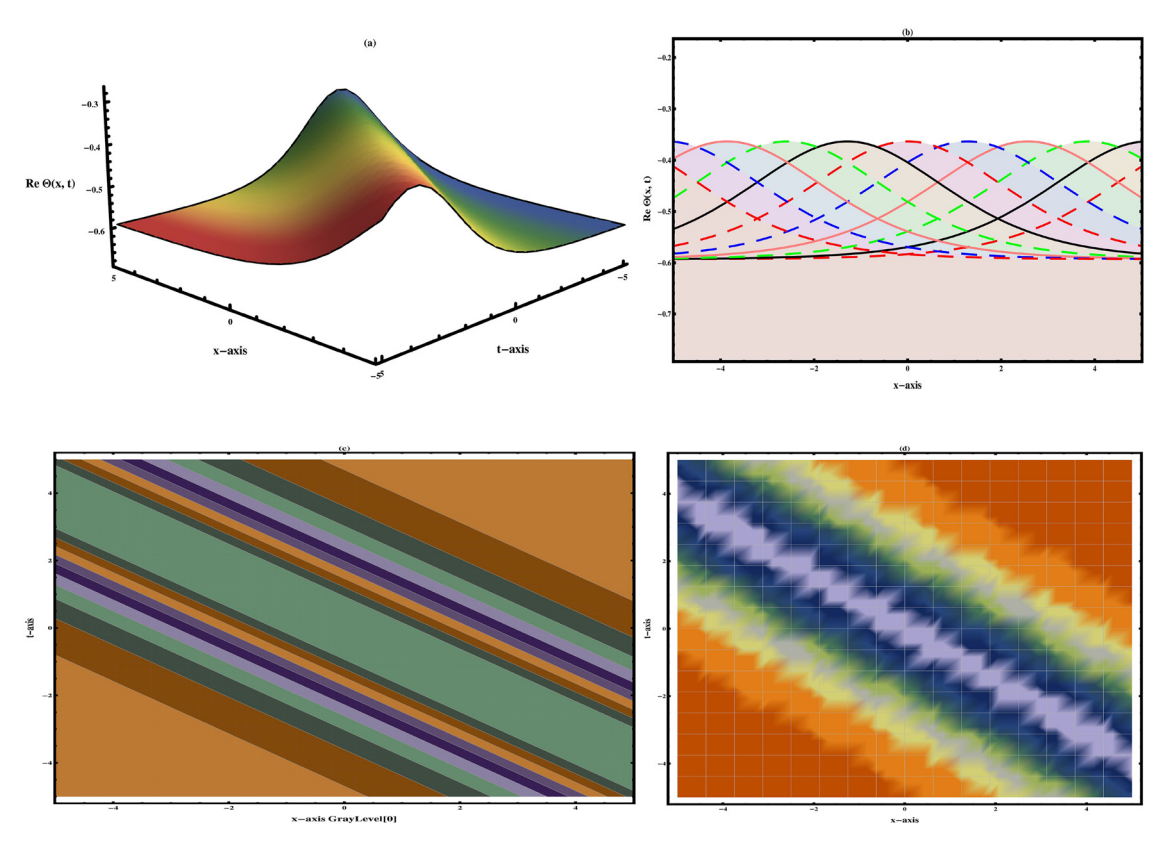


Figure 17: Visualization of Eq. (44) shows the bright wave structure under different arbitrary values k = 0.4, $\beta = 0.5$, $\vartheta = 0.6$, and $\gamma = 0.2$, at $\alpha = 0.98$.

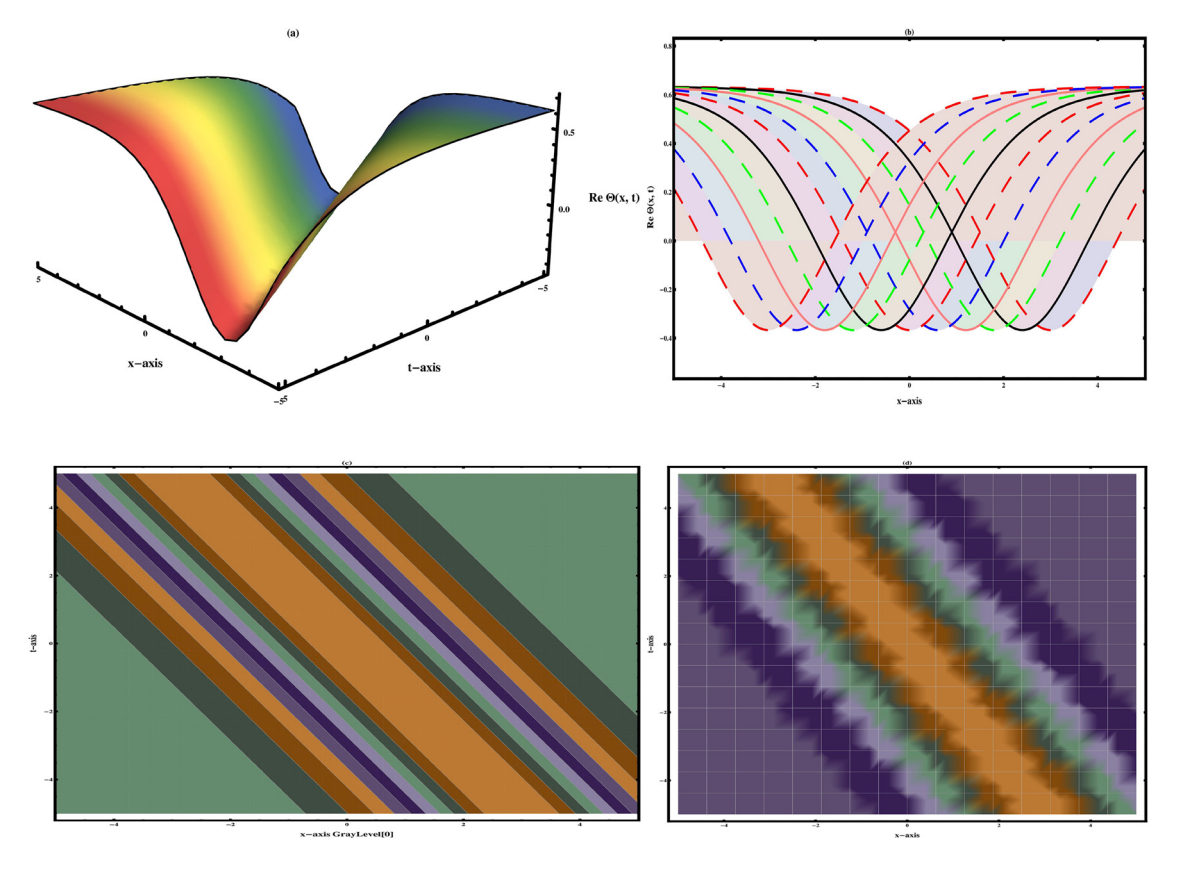


Figure 18: Visualization of Eq. (47) shows the dark wave structure under different arbitrary values k = 0.5, $\beta = -0.6$, $\vartheta = 0.3$, and $\gamma = 0.4$, at $\alpha = 0.96$.

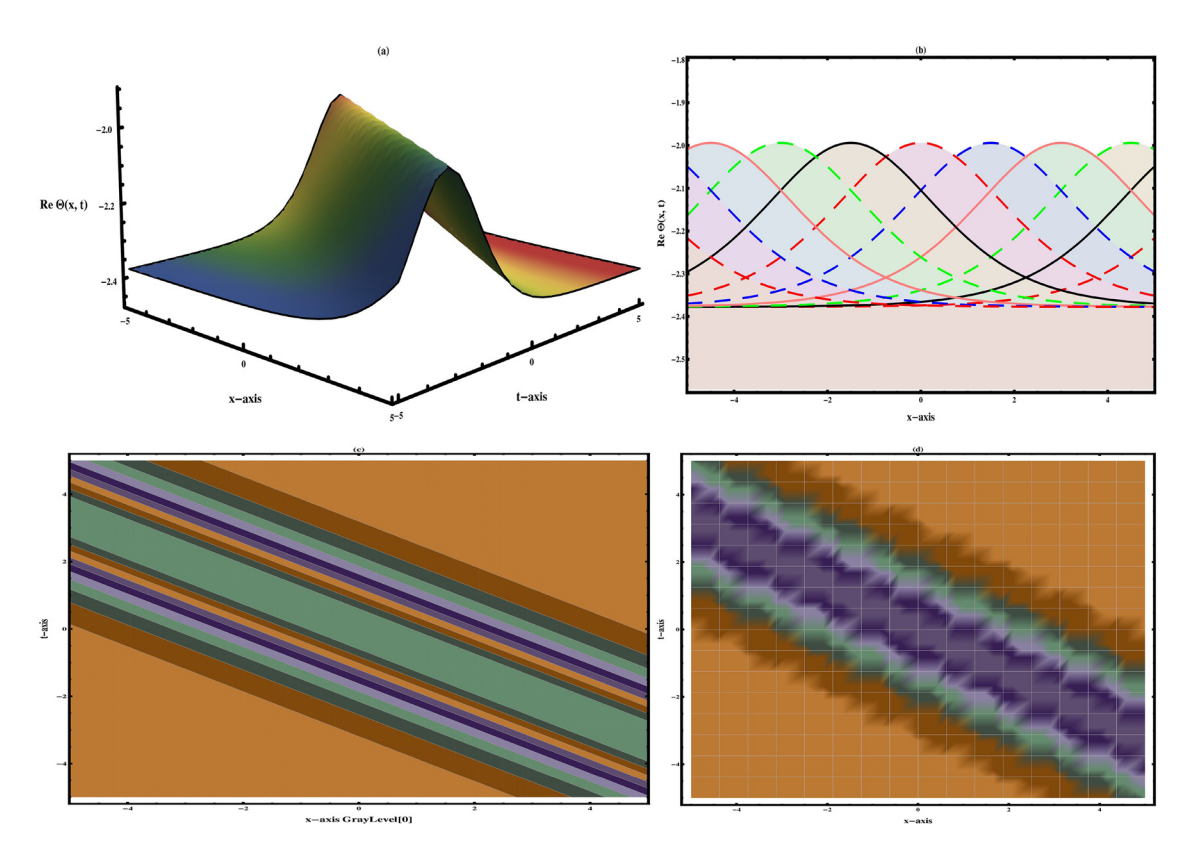


Figure 19: Visualization of Eq. (50) shows the exponential wave structure under different arbitrary values k = 0.7, $\beta = 1.6$, $\vartheta = 0.9$, and $\gamma = 0.5$, at $\alpha = 0.99$.

 $2\beta\mu q_0 W_{xx} + 2\beta\mu^2 W_x^2 + 2\beta\mu^2 W W_{xx} + \gamma\mu W_{xxxx} + \mu W_{tt} = 0. (56)$ On linearizing Eq. (56) in terms of μ , we retrieve

00 717 717 0 4--

$$2\beta \mu q_0 W_{xx} + \gamma \mu W_{xxxx} + \mu W_{tt} = 0.$$
 (57)

For further proceeding, we take the solutions of Eq. (57) as

$$W(x,t) = \lambda e^{i(lx+t\Omega)}, \tag{58}$$

where the normalized wave number and frequency of perturbation are denoted by l and Ω , respectively.

By inserting Eq. (58) into Eq. (57), we have

$$-\gamma l^4 + 2\beta l^2 q_0 + \Omega^2 = 0. {(59)}$$

The dispersion relation, in terms of Ω is as follows:

$$\Omega = \sqrt{\gamma l^4 - 2\beta l^2 q_0}. \tag{60}$$

The dispersion relation obtained in Eq. (60) is illustrated in Figure 9. If the wave number Ω is imaginary, meaning perturbations grow exponentially, the steady state solution becomes unstable. Alternatively, if Ω has a real value, indicating stability against small perturbations and the steady state remains stable. The sign of Ω indicates whether the solution will amplify or diminish with time. A Ω_{max} of

precisely 0 indicates that the steady state solution is slightly stable.

7 Results and discussion

In this section, we discuss the outcomes of our proposed model and provide physical interpretations. It focuses on finding interesting, more generalized, and novel exact wave structures, including hyperbolic, trigonometric, complex hyperbolic, rational, bright, dark, singular, and singular periodic wave behaviors. Dark solitons exhibit greater stability and resistance to signal degradation

Table 1: Comparative study (Novelty)

References	Soliton solutions	Stab. analysis	SA	Bifur. analysis
In [23]	Yes	No	No	No
In [24]	Yes	No	No	No
In [25]	Yes	No	No	No
In [26]	Yes	No	No	No
In current study	Yes	Yes	Yes	Yes

compared to conventional solitons, despite their higher complexity in control. Bright solitons, meanwhile, are exemplified by their highest intensity, which surpasses the surrounding background levels. Another type, singular solitons, features abrupt discontinuities – often infinite – and may correspond to solitary waves with imaginary central positions. These singular shapes are particularly substantial in modeling rogue wave phenomena, where sudden, extreme amplitude spikes emerge. Moreover, periodic wave solutions characterize oscillatory forms that repeat at regular intervals, administrated by their wavelength and frequency. The period (time for one full cycle) and frequency (cycles per second) are defining parameters of such waveforms. These solutions have distinct physical interpretations, and we illustrate them graphically by choosing appropriate parameter values. These outcomes serve as inspiration for further research across different scientific fields, particularly in fluid dynamics. In the recent past, intensive work has been done on a given model. Li [23] retrieved solutions through the trial equation method. Taghizadeh et al [24] found exact traveling solutions with the aid of the homogeneous balance method. Kaplan et al. [25] discussed exact solutions and conservation laws *via* $\exp(-\Phi(\xi))$ -expansion method and multiplier approach. Zhen et al. [26] attained diverse forms of exact traveling wave solutions by employing an improved projective Riccati equation method. However, in this study, by employing the extended NEDAM, GAM and ansatz methods, we have generated numerous solitary pulse solutions. These solutions are practical, concise, and easily comprehensible, making them valuable for applications in fluid dynamics, ocean engineering, and other deepwater nonlinear phenomena. Moreover, our solutions provide insights for further investigation into higher-order NLPDEs. Graphical representation is essential for accurately depicting nonlinear events and relationships between variables in a dataset. The accompanying 2D, 3D, and contour plots in Figures 10-19. visually demonstrate the solutions obtained, facilitating a clearer understanding of problem-solving approaches. These graphical representations are effective tools for conveying complex concepts and methodologies in nonlinear wave analysis. The graphics below depict our BO model with fractional derivatives. The results of this study hold noteworthy implications across multiple physics domains. The hyperbolic tangent function proves crucial for computing magnetic moments and relativistic rapidity, while the hyperbolic secant accurately models velocity profiles in laminar jets. Besides, the hyperbolic cotangent displays a direct relationship with the Langevin function, an important tool for evaluating magnetic polarization. These findings highlight the

central role of hyperbolic functions in modeling various physical systems. The results computed in this study have significant physical implications, particularly in the context of soliton theory and applications in others fields of applied sciences such as physics, electrical engineering, control theory, and wave phenomena. Furthermore, computed solutions and dynamical analyses, such as bifurcation analysis, and SA have diverse real applications across multiple fields. Solitons, which are stable, localized waves that maintain their shape over long distances, are crucial in optical fiber communications for transmitting data pulses without distortion, as well as in hydrodynamics for modeling tsunamis and tidal bores. Bifurcation analysis helps understand sudden changes in system behavior, such as in mechanical engineering for predicting structural buckling, in ecology for studying population dynamics under environmental stress, and in electrical engineering for analyzing voltage collapses in power grids. SA quantifies how variations in input parameters affect outputs, making it essential in climate modeling to assess the impact of different factors on global warming, in pharmacokinetics to optimize drug dosages, and in financial risk management to evaluate portfolio vulnerabilities. Together, these mathematical tools enhance the modeling, prediction, and optimization of complex systems in science and engineering. The results extracted are exceptional and novel in comparison to previous findings in the literature. We briefly compare our obtained solutions with those presented in earlier research. Our findings lead to the following conclusions, presented in tabular form, which highlight the novelty of the present work (Table 1).

8 Concluding remarks

This study has investigated new exact traveling wave patterns for the time-FBO equation by using three efficient suggested computational techniques. These methods help us to uncover various exact solutions, including trigonometric, bright, dark singular, exponential, and their combined complex forms. We also observe singular periodic, plane-wave, and exponential solutions. Furthermore, we conduct stability analysis on the governed BO equations, confirming their high stability. Also, by amalgamating sensitivity, bifurcation, and stability analyses into our study, we can gain deeper insights into the behavior of the FBO equation and further authenticate the efficiency of the applied methodologies. The enduring stability of solitons, demonstrated as soliton pulses, travel through ideal lossless nonlinear fibers, mathematical physics, fluid

dynamics, ocean engineering, and other deep-water nonlinear phenomena and highlight their potential integration into complex communication systems. We validate our results using Mathematica software, visually representing certain wave structures through 2D, 3D, contour, and density graphs with appropriate parameter values. Our findings illustrate the effectiveness of these aforementioned approaches in enhancing nonlinear dynamical behavior and suggest their potential application in uncovering diverse and novel soliton solutions for other NLPDEs encountered in mathematical physics and engineering. Through a comparative analysis of our newly developed solutions, it becomes evident that our proposed methods offer several advantages. They demonstrate strength, reliability, ease of implementation, and efficiency when applied to various NLPDEs. This makes it superior to previously utilized methods. The solutions obtained in this study will serve as a foundation for enhancing our understanding of water wave propagation in both shallow and deep water. This study displays a robust and methodical method for solving nonlinear fractional problems, leading to the discovery of novel exact solutions. Moving forward, we aim to expand the method's versatility, with a concentration on tackling highly nonlinear systems, variable-coefficient models, and variable-order FPDEs. Furthermore, we will plan: (i) to extend these methodologies to other nonlinear fractional PDEs or consider higher-dimensional generalizations; (ii) to analyze the effects of noise term by adding the stochastic term in the governing equation; and (iii) to develop new numerical and analytical methods to solve FBO equations, enabling more accurate and efficient simulations.

DE GRUYTER

Acknowledgments: The authors extend their appreciation to Taif University, Saudi Arabia, for supporting this work through project number (TU-DSPP-2024-70).

Funding information: This research was financially supported by Firat University.

Author contributions: Muhammad Bilal: methodology, software, and writing - original draft. Shafqat Ur Rehman: investigation, conceptualization, and writing - review and editing. Usman Younas: data curation, writing - review and editing, and visualization. Alsharef Mohammad: formal analysis, conceptualization, and funding acquisition. Shahram Rezapoure: formal analysis, data curation, and conceptualization. Mustafa Inc: resources, validation, and writing – review and editing. All authors have accepted responsibility for the entire content of this manuscript and approved its submission.

Conflict of interest: The authors state no conflict of interest.

Data availability statement: All data generated or analyzed during this study are included in this published article.

References

- Mandal UK, Malik S, Kumar S, Das A. A generalized (2+1)dimensional Hirota bilinear equation: integrability, solitons and invariant solutions. Nonlinear Dvn. 2023:111(5):4593-611.
- Ying L, Li M, Shi Y. New exact solutions and related dynamic [2] behaviors of a (3+1)-dimensional generalized Kadomtsev-Petviashvili equation. Nonlinear Dyn. 2024;112(13):11349-72.
- Rezazadeh H, Younis M, Eslami M, Bilal M, Younas U. New exact traveling wave solutions to the (2+1)-dimensional Chiral nonlinear Schrödinger equation. Math Model Nat Phenom. 2021;16:38.
- Eslami M, Rezazadeh H. The first integral method for Wu-Zhang [4] system with conformable time-fractional derivative. Calcolo. 2016;53(3):475-85.
- Wang KJ, Shi F, Wang GD. Abundant soliton structures to the (2+1)-[5] dimensional Heisenberg ferromagnetic spin chain dynamical model. Adv Math Phys. 2023;2023(1):4348758.
- [6] Bilal M, Seadawy AR, Younis M, Rizvi STR, Zahed H. Dispersive of propagation wave solutions to unidirectional shallow water wave Dullin-Gottwald-Holm system and modulation instability analysis. Math Methods Appl Sci. 2021;44(5):4094-104.
- Guan X, Liu W, Zhou Q, Biswas A. Darboux transformation and analytic solutions for a generalized super-NLS-mKdV equation. Nonlinear Dyn. 2019;98(2):1491-500.
- [8] Alruwaili AD, Seadawy AR, Igbal M, Beinane SAO. Dust-acoustic solitary wave solutions for mixed nonlinearity modified Kortewegde Vries dynamical equation via analytical mathematical methods. J Geom Phys. 2022;176:104504.
- Bilal M, Ren J, Inc M, Algahtani RT. Dynamics of solitons and weakly ion-acoustic wave structures to the nonlinear dynamical model via analytical techniques. Opt Quantum Electron. 2023;55(7):656.
- Wang XB, Han B. Application of the Riemann-Hilbert method to the vector modified Korteweg-de Vries equation. Nonlinear Dyn. 2020;99(2):1363-77.
- Hussain A, Ibrahim TF, Birkea FMO, Al-Sinan BR. Dynamical behavior of analytical soliton solutions to the Kuralay equations via symbolic computation. Nonlinear Dyn. 2024;112(22):20231-54.
- Usman M, Hussain A, Abd El-Rahman M, Herrera J. Group theoretic approach to (4+1)-dimensional Boiti-Leon-Manna-Pempinelli equation. Alex Eng J. 2025;118:449-65.
- [13] Hussain A, Zaman FD, Ali H. Dynamic nature of analytical soliton solutions of the nonlinear ZKBBM and GZKBBM equations. Partial Differ Equ Appl Math. 2024;10:100670.
- Jumarie G. Laplace's transform of fractional order via the Mittag-Leffler function and modified Riemann-Liouville derivative. Appl Math Lett. 2009;22(11):1659-64.
- Mozaffari FS, Hassanabadi H, Sobhani H, Chung WS. On the conformable fractional quantum mechanics. J Korean Phys Soc. 2018;72(9):980-6.
- Cevikel AC. Traveling wave solutions of conformable Duffing model in shallow water waves. Int J Mod Phys B. 2022;36(25):2250164.

- [17] Chen C, Jiang YL. Simplest equation method for some timefractional partial differential equations with conformable derivative. Comput Math Appl. 2018;75(8):2978–88.
- [18] Kumar D, Kaplan M. New analytical solutions of (2+1)-dimensional conformable time fractional Zoomeron equation via two distinct techniques. Chin J Phys. 2018;56(5):2173–85.
- [19] Benjamin TB. Internal waves of permanent form in fluids of great depth. I Fluid Mech. 1967:29(3):559–92.
- [20] Ono H. Algebraic solitary waves in stratified fluids. J Phys Soc Jpn. 1975;39(4):1082–91.
- [21] Ewen JF, Gunshor RL, Weston VH. Surface acoustic solitons. Jpn J Appl Phys. 1980;19(S1):683.
- [22] Sagar B, Ray SS. A localized meshfree technique for solving fractional Benjamin-Ono equation describing long internal waves in deep stratified fluids. Commun Nonlinear Sci Numer Simul. 2023:123:107287.
- [23] Li Y. Application of Trial Equation Method for Solving the Benjamin Ono Equation. J Appl Math Phys. 2014;2(3):45–9.
- [24] Taghizadeh N, Mirzazadeh M, Farahrooz F. Exact soliton solutions for second-order Benjamin-Ono equation. Appl Appl Math Int J. 2011;6(1):31.
- [25] Kaplan M, San S, Bekir A. On the exact solutions and conservation laws to the Benjamin-Ono equation. J Appl Anal Comput. 2018;8(1):1–9.
- [26] Zhen W, De-Sheng L, Hui-Fang L, Hong-Qing Z. A method for constructing exact solutions and application to Benjamin Ono equation. Chin Phys. 2005;14(11):2158.
- [27] Tasbozan O. New analytical solutions for time fractional Benjamin-Ono equation arising internal waves in deep water. China Ocean Eng. 2019;33(5):593–600.
- [28] Mirhosseini-Alizamini SM, Rezazadeh H, Srinivasa K, Bekir A. New closed form solutions of the new coupled Konno-Oono equation using the new extended direct algebraic method. Pramana. 2020;94(1):52.

- [29] Bhan C, Karwasra R, Malik S, Kumar S. Bifurcation, chaotic behavior, and soliton solutions to the KP-BBM equation through new Kudryashov and generalized Arnous methods. AIMS Math. 2024;9(4):8749–67.
- [30] Park C, Nuruddeen RI, Ali KK, Muhammad L, Osman MS, Baleanu D. Novel hyperbolic and exponential ansatz methods to the fractional fifth-order Korteweg-de Vries equations. Adv Differ Equ. 2020:2020(1):12.
- [31] Bilal M, Ahmad J. New exact solitary wave solutions for the 3D-FWBBM model in arising shallow water waves by two analytical methods. Results Phys. 2021;25:104230.
- [32] Zulfiqar A, Ahmad J. Exact solitary wave solutions of fractional modified Camassa-Holm equation using an efficient method. Alex Eng J. 2020;59(5):3565–74.
- [33] Rehman SU, Bilal M, Ren J, Bayram M, Inc M. Sensitivity Analysis and Dynamics of Optical Dromions in Conformable Generalized Nonlinear Schrödinger Systems. Phys Lett A. 2024;531:130168.
- [34] Lu W, Ahmad J, Akram S, Aldwoah KA. Soliton solutions and sensitivity analysis to nonlinear wave model arising in optics. Phys Scr. 2024;99(8):085230.
- [35] Islam SR, Khan K, Akbar MA. Optical soliton solutions, bifurcation, and stability analysis of the Chen-Lee-Liu model. Results Phys. 2023;51:106620.
- [36] ur Rahman M, Sun M, Boulaaras S, Baleanu D. Bifurcations, chaotic behavior, sensitivity analysis, and various soliton solutions for the extended nonlinear Schrödinger equation. Bound Value Probl. 2024;2024(1):15.
- [37] Alazman I, Alkahtani BST, Mishra MN. Dynamic of bifurcation, chaotic structure and multi soliton of fractional nonlinear Schrödinger equation arise in plasma physics. Sci Rep. 2024;14(1):25781.
- [38] Ali A, Ahmad J, Javed S. Stability analysis and novel complex solutions to the malaria model utilising conformable derivatives. Eur Phys J Plus. 2023;138(3):259.